The Mandibular Canal at the Region of the Molar Teeth:
An Evaluation of Cone Beam Volumetric Tomography

Hai Ngoc Nguyen, *DDS*

A treatise submitted in fulfillment of the requirements
for the degree of
Master of Science in Dentistry
of The University of Sydney

Department of Oral and Maxillofacial Surgery
Faculty of Dentistry
The University of Sydney

2008

ABSTRACT

Objectives: The aims of this study were:

- to evaluate the exact level of the mandibular canal using Cone Beam Volumetric Tomography (CBVT) using measurements taken on images from the NewTom3G and i-CAT machines and manually
- to determine the course of the mandibular canal in the regions of the first, second , and third molars
- to compare the course of the mandibular canals bilaterally
- to compare variables measured between the CBVT and panoramic units
- to determine appropriate positions for the implant placement at the region of the mandibular molars in relation to the mandibular canal.

Methods: Ten mandibles were selected, including seven edentulous and three dentate ones. They were marked at four positions from the distal border of the mental foramina in the posterior direction at intervals of 10.00 mm. On each dry mandible, at four sites namely M_0, M_1, M_2, and M_3, Gutta Percha (GP) points, known as markers, were attached to the mandible so that they were parallel to the midline of the mandible on both buccal and lingual sides. On the NewTom 3G and i-CAT, variables of cross-sectional images were measured from the alveolar crest of the mandible to the superior border of the mandibular canal (AC); the lingual rim of the canal to the lingual margin of the mandible (LC); the buccal rim of the canal to the buccal margin of the mandible (BC); the inferior rim of the canal to the lower border of the mandible (IC), and from the lingual margin to the buccal margin of the mandible (BW: Bone Width). Dry mandibles were subsequently sacrificed by cutting at the four marked sites. On each cross-section of mandibles, distances AC, BC, LC, IC, and BW were measured using a caliper as the manual measurement. IC distances on a conventional Orthophos

panoramic machine were also measured to compare with the CBVT. Data were managed by Microsoft Office Excel 2003 and transferred to the software of Statistics Package for Social Sciences (SPSS) version 15.0 for Windows for analysis. Data were presented as Mean, Standard Deviation (SD), and Mean Difference, and Standard Error of Mean (SEM) with decimal at 0.00. T-test and One-way ANOVA were used to analyse variables measured in which T-test was used to analyse variables with paired samples and One-way ANOVA was used with adjustment for multiple comparisons of Bonferroni. Statistical significance has an assumed P- value of 0.05 or less.

Results: The findings showed that there was no significant difference among measured variables from the NewTom 3G, i-CAT and manual measurement ($P>0.05$). There was significant statistical difference between the Orthophos OPG machine and CBVT system ($P=0.00<0.05$). There was no significant difference in the course of the mandibular canals bilaterally ($P>0.05$). On average, Distances AC, BC, LC, and IC were obtained for reference purposes. The bone width of the mandible on the right side was slightly different from that on the left side.

Conclusions: The findings implied CBVT was an accurate diagnostic tool for locating the course of the mandibular canal and for placing dental implants in the region of the mandibular molars. The course of the mandibular canal on the left and right sides was variable. The distances measured at the region of the first, second, and third mandibular molars should be considered as a valuable reference. The bone width of the mandible on the right and left sides was slightly different. The accuracy of the NewTom3G and i-CAT was superior to the panoramic Orthophos machine. However, a panoramic radiograph is still valuable in the daily dental clinic.

Key words: Cone Beam Volumetric Tomography (CBVT), mandibular canal, molar region.

DEDICATION

This work is dedicated to my parents who have sacrificed their whole life to bring their children up to become educated people, and to my wife Ha and our two daughters Quynh Anh and Ha My who have suffered because of me being far away. They have supported to me in a loving way during my years of studying in Australia. Also, this dedication goes to my brothers and sister who, from childhood to now, have shared their support and love with me.

ACKNOWLEDGEMENTS

I am greatly indebted to my supervisors, Dr. Malcolm Iain Coombs, Head of The Oral Surgery and Diagnostic Imaging Department, Sydney Dental Hospital, Australia, Conjoint Associate Professor of The University of Newcastle, and Dr. Antonia Maree Scott, Head of The Discipline Oral Diagnosis and Oral Radiology, Faculty of Dentistry, The University of Sydney, Australia, for their advice, guidance, support, encouragement, and inspiration throughout the full challenge of the path to complete this study.

I am also grateful to Associate Professor Christopher Peck, Pro-Dean of the Faculty of Dentistry, who has given valuable encouragement to my study, creating a lever force to motivate and inspire me in pursuing the way to obtain my target.

I would like to express my great appreciation to Mrs. Heather Coombs who spent much time proof reading and editing this study.

All help from Mrs. Rebecca Granger, Postgraduate Studies Officer, is greatly acknowledged.

I wish to thank the Sydney Dental Hospital Board, who has allowed me to work in the hospital environment, and especially once again thank Dr. Malcolm I Coombs, my supervisor, who, with his expert knowledge, has dedicated much time to help me to enrich my knowledge, particular in the field of CBVT, and also how to use the NewTom3G system.

Thanks are due to the staff of the Oral Diagnosis and Radiology Unit, Westmead Centre of Oral Health, Australia, especially Mr. Bruce Waters, senior radiographer, Head of the Unit and Mr. Jason Chua, medical radiographer, for all their enthusiastic guidance in the use of the i-CAT system, contributing an important part of this study.

I would like to express my sincerest appreciation to Dr. Antonia M. Scott, Dr. Malcolm I. Coombs, Mr. Hugh McCuaig, Faculty Manager, and Mrs. Penny Bayl, Administrative Sevices Officer, who have given me an opportunity to work in a high academic environment that has greatly improved my academic skills.

Special thanks go to all staff of the Oral Surgery and Diagnostic Imaging Department, Sydney Dental Hospital, New South Wales, Australia, especially Mr. Albert Ho, Dr. Amelita Simpson, Mrs. Christina Stucci, Mrs. Diane Nikolic, Mrs. Luisa Berroya, and Mrs. Susan Baker for all their help, enthusiasm, and support. Also, I wish to thank Mr. Luu Van, Information Technology (IT) Department, Sydney Dental Hospital, for all his help.

I would like to thank Mr. Jeremy Cullis, Dental Librarian, the Faculty of Dentistry, for his enthusiastic guidance in the use of IT techniques in searching for articles and materials, and particularly in the use of Endnote software in my early days of stepping into the university environment.

I am grateful to the Department of Medical Anatomy of the University of Medicine and Pharmacy, Ho Chi Minh City, Vietnam from where the dry mandibles were obtained.

I would like to thank the Vietnam Government and my employer, the Faculty of Dentistry, the University of Medicine and Pharmacy, Ho Chi Minh City, Vietnam, for awarding me a master scholarship to study at the University of Sydney, Australia. I also wish to thank the Faculty of Dentistry, the University of Sydney, Australia, for allowing me to study here.

LIST OF PUBLICATIONS

Proceedings

1. H. N. Nguyen, A. M Scott, M. I. Coombs, and A. Simpson. The mandibular canal at the region of the molar teeth: an evaluation of CBVT. The 11th Congress of the European Academy of Dento-Maxillo-Facial Radiology. (25-28 June), 2008 Budapest, Hungary.
2. H. N. Nguyen, A. M Scott, and M. I. Coombs. Accuracy of CBVT imaging of the mandibular canal; comparison with panoramic radiology. The 48th Annual Meeting of the ANZ IADR (October 1-3, 2008), Perth, Australia.

Posters

1. H. N. Nguyen, A. M. Scott, M. I. Coombs, and A. Simpson. The mandibular canal at the region of molar teeth: an evaluation of CBVT. Annual Research Day, Faculty of Dentistry, The University of Sydney, Australia. 4th July, 2008. (Exempted with the approval of Prof. Greg Murray, the post-coordinator, Faculty of Dentistry, because at that time the author attended The 11th Congress of the European Academy of Dento-Maxillo-Facial Radiology. (25-28 June), 2008 Budapest, Hungary.
2. H. N. Nguyen, A. M. Scott, and M. I. Coombs. Accuracy of CBVT imaging of the mandibular canal; comparison with panoramic radiology. The 48th Annual Meeting of the ANZ IADR (1-3 October 2008), Perth, Australia. The abstract for the poster presentation was accepted, but, after reviewing, it was suggested that an oral presentation be given.

Papers

1. H. N. Nguyen, A. M Scott, M. I. Coombs, and A. Simpson. The mandibular canal at the region of the molar teeth: an evaluation of CBVT. Oral Radiology, submitted (Nov. 2008).

ABBREVIATIONS

AC : the distance measured from the alveolar crest of the mandible to the superior border of the mandibular canal

BC : the distance from the buccal rim of the mandibular canal to the buccal margin of the mandible

BERT: : Background Equivalent Radiation Time

BW : Bone Width - the distance from the lingual margin to buccal margin of the mandible

CBCT : Cone Beam Computed Tomography

CBVI : Cone Beam Volumetric Imaging

CBVT : Cone Beam Volumetric Tomography

CCD : Charge-Coupled Device

CI : Confidence Interval

CT : Computed Tomography

DICOM : Digital Imaging and Communications in Medicine

FOV : Field Of View

GP : Gutta Percha

IAN : Inferior Alveolar Nerve

IANB : Inferior Alveolar Nerve Bundle

IC : the distance from the inferior rim of the mandibular canal to the lower border of the mandible

ICRP : International Commission on Radiation Protection

L : Left

LC : the distance from the lingual rim of the mandibular canal to the lingual margin of the mandible

LED : Light Emitting Diode

MDCT : Multidetector CT

MRI : Magnetic Resonance Imaging

µSv : micro Sieverts

R : Right

SD : Standard Deviation

SEM : Standard Error of Mean

SPSS : Statistics Package for Social Sciences

TMJ : TemporoMandibular Joint

TABLE OF CONTENTS

Contents **Pages**

Chapter 1

INTRODUCTION AND LITERATURE REVIEW

I. INTRODUCTION

The provision of implants in the posterior mandible has become a popular choice in the dental care for an ageing affluent society. Furthermore, missing mandibular molars have created oral health problems in the community and the demand for rehabilitation through implantology of missing teeth of this region has rapidly increased in dental clinical practice. On the other hand, the mandibular canal is one of the most important anatomic structures about which surgeons need to have a detailed knowledge to order to prevent damaging the inferior alveolar nerve (IAN) which could lead to post-surgery neurosensory disturbance [1].

Some studies associated with the mandibular neurovascular canal have based their evaluation on modalities such as panoramic tomography, Computed Tomography (CT), Magnetic Resonance Imaging (MRI), and Cone-Beam Volumetric Tomography (CBVT). The term CBVT is interchangeable with Cone-Beam Computed Tomography (CBCT) and Cone-Beam Volumetric Imaging (CBVI). CBVT is the term chosen for this treatise.

Panoramic tomography can reveal the mandibular canal on both left and right sides and is considered the primary radiograph for oral diagnosis. In addition, a vertical distance from the alveolar crest to the superior border of the mandibular canal can be measured for a pre-surgical assessment with calibration corrected for magnification that is approximately 25 to 30% of real structures. However, in panoramic tomography it is

impossible to display the image of the mandibular canal in the bucco-lingual direction. Image structures on a panoramic radiograph can be magnified and/ or distorted due to incorrect patient positioning.

Previously, with MRI, there have been some studies associated with the mandibular canal [2, 61, 62]. MRI imaging is excellent for visualizing soft-tissue structures in that the inferior alveolar neurovascular bundle (IANB) can easily be visualized on images in other planes, such as cross-sectional and panoramic reformations. However, a disadvantage of MRI is that spatial distortions are probably larger than those of CT and this may lead to limited use of this technique [2]. Visualization of bone structure in MR images is low or even without any signal, but bone structures can differ from the surrounding soft tissues providing that the high intensity signal (T1-Weight) is used.

For CT, Klinge et al [3] reported that conventional CT was an accurate diagnostic tool to localize the position of the mandibular canal when compared with periapical and panoramic radiographs. At the time of his research, CT appeared to be the best choice. However, the issue discussed here is that the angles of designed implants at the region of the mandibular molars frequently differ from the angle perpendicular to the axial CT plane and the measurement is often inaccurate [4]. Thus, for the conventional CT, the patient's head position is important. In correct patient positioning, the spiral helixes will be parallel to the occlusal plane of the jaw. An image distortion may occur if patient positioning is not ideal. The radiation dose of conventional CT to the maxillofacial region is considered very high (page33).

At present, CBVT is emerging as an accurate tool of imaging diagnosis for dental clinical applications relating to fields of oral surgery, implantology, periodontology, temporomandibular joint (TMJ) imaging and orthodontics [5, 69, 70] due to its advantages of image accuracy, low radiation dose, and rapid time. With a two dimensional detector, CBVT can capture the whole structure of the region of interest by operating a single 360^{o} rotation of the gantry [6], while conventional CT scanners must scan multiple slices which are then stacked together to obtain a final image [5].

In summary, it is essential to assess the correlation between a dental implant placement and the IAN to avoid unexpected injury as well as to ensure a successful outcome. To the author's knowledge, an evaluation of the course of the mandibular canal, in relation to the sites in the region of the first, second, and third molars, based on the analysis of the CBVT system, has not yet been carried out. This study was undertaken to address it.

In the present study, an assessment of the course of the mandibular canal at the region of the lower molars was carried out with data from the CBVT and conventional panoramic systems. The aims of this study are to:

- Evaluate the level of accuracy of the CBVT system by analysis variables measured from the NewTom 3G and i-CAT machines
- Determine the correlation of the mandibular canal in the regions of the first, second, and third molars within the body of the mandible
- Compare the course of the mandibular canal on the left and right sides
- Compare variables measured between the CBVT system and the conventional panoramic unit

- Determine the possibility of appropriate positions for implant placement at the region of the molars in relation to the mandibular canal.

II. LITERATURE REVIEW

1. The mandibular canal

1.1. Anatomy of the course of the mandibular neurovascular canal

The mandibular nerve passes from the trigeminal ganglion through the foramen ovale forwards and downwards to the medial surface of the ramus of the mandible. It enters the mandibular canal through the mandibular foramen where it continues to exit via the mental foramen. Before entering the mandible, it divides to supply the tongue and soft tissues of the cheek. After passing through the mandibular foramen, its name is changed to the inferior alveolar nerve (IAN). The IAN contains mainly sensory fibres and a few motor fibres distributed by the mylohyoid nerve to the mylohyoid and the anterior belly of the digastric muscles [7]. Inside the mandibular canal, the IAN, which is approximately 4mm in diameter [8], then runs forwards accompanied by the inferior alveolar vessels to establish the inferior alveolar neurovascular bundle (IANB). The IAN innervates the lower premolars and molars and adjacent parts of the gingiva. Its terminal branch emerges from the mental foramen and becomes the mental nerve which, in turn, innervates the skin of the chin and the lower lip, while the smaller incisive branch continues through the bone to innervate the canine and incisor teeth.

In most cases, the IAN is a single trunk with several sub-branches upwards to the superior border of the mandible [9]. It passes along the mandible and lies above the lower one-third of the body of mandible and about 4.5 to 5 mm below the mental foramen [10]. However, according to Kieser et al, the mandibular canal is located in the lower half of the mandible in 73% of males and 70% of females. This indicates no significant difference between males and females [9]. Additionally, the mandibular canal is mostly located at the buccal aspect of the roots in the bucco-lingual direction [11, 12]. Brooks et al reported that when using the i-CAT machine, the mandibular canals of humans were more easily visible than those of the cadavers. This could be attributed to the age of the specimens or the effect of the thawing process [116].

Generally, the course of the IANB is clearly described in terms of anatomy. However, its course is quite variable and it does not maintain a constant position in the mandible [7, 13]. Thus, in this study, a scrutiny of the course of the mandibular canal was carried out to corroborate previous studies.

1.2. The injury risk to the inferior alveolar nerve

An injury of the IAN can lead to the paraesthesia/ anaesthesia of the lower lip and chin [7]. There are several causes associated with the injury of the IAN. These include benign or malignant tumours in the mandible, orthognathic surgery, endodontic treatment, the removal of the mandibular third molars, placement of implants, and sliding osteotomy. Sensory dysfunction of the IAN may recover completely, depending on the injury level, usually taking from one month to one year [14].

The injury incidence of the IAN ranges from 0.4 to 5.5% in which permanently damaged IAN accounted for 0.3 to 0.9% [15]. Ellies et al reported that there was 37% of sensory dysfunction one month after placing dental implants, and 13% more than 6 months later [16]. Similarly, van Steenbergher et al [17] reported that there was 6.5% of sensory dysfunction of the IAN a year after placing implants in the region of the mandibular molars.

According to dental literature, a close relationship between the mandibular canal and the roots of the first and second molars is quite rare, particularly the distal roots [18]. However, in a few cases, there could be sensory dysfunction of the IAN, particularly if the roots of the first and second molars are enlarged and this is not diagnosed prior to treatment. Farronato el al [18] reported the following clinical case.

A patient came to the department with sensory dysfunction of the lower lip that had occurred about 6 months after orthodontic appliances were used to move the first and second molars distally. Unfortunately, the movement of a long and large root of the lower second molar damaged the mandibular canal that led to the sensory dysfunction of the lip and chin on the same side. By removing the orthodontic appliances and using oral medications, the patient did not suffer any further paraesthesia. In the primary treatment of this case, only a panoramic radiograph was taken. This had limitations for diagnosis and this unexpected result could not have been predicted.

In endodontic treatment, an injured IAN can derive from physical or chemical factors. Overfilling sealers or medicament of the root canals, in which calcium hydroxide and formaldehyde are used, are considered the main causes [19-21] that could lead to IAN paraesthesia. Yatsuhashi et al preferred to use microscopic endodontic treatment

combined with the physiological saline solution and vitamin B12 to recover the function of the IAN [22].

Additionally, injury of the IAN can occur in orthognathic surgery in split ramus osteotomy of the mandible. According to Tsuji et al, for sagittal split ramus osteotomies of the mandible, the position anterior to the mandibular angle is considered as one of the safest locations for the IAN when performing buccal corticotomy [23]. Computed tomography (CT) was considered the best choice to evaluate the position and course of the mandibular canal for this procedure [23].

Further contributing to possible sensory dysfunction of the IAN are the limitations of traditional two-dimensional radiographs such as the image magnification, distortion and the lack of information in the bucco-lingual direction. For this, a pre-surgical assessment with three-dimensional imaging should be strongly recommended to avoid or reduce post-operative injury of the IAN.

The injury risk of the IAN is reduced significantly when extracting impacted mandibular molars providing that CT images are used for the pre-operative examination rather than using only panoramic tomography. Three-dimensional imaging more exactly provides information about the relationship between the impacted mandibular molar and the mandibular canal. For example, Susarla et al [24] reported that in reviewing panoramic tomograms, 80.4% of third molars evaluated were considered to be at high risk of IAN injury. However, only 32.6% of the same sample were considered to have a potential high risk to IAN injury when visualized on the CT. It is clear that the CT has more significance in diagnosing the relationship of the mandibular canal and impacted mandibular molars than the panoramic system.

Todd et al [25] reported that the visualization of the mandibular canal on the CT was much clearer than that of panoramic tomography. Hanazawa et al also realized that either the CT or CBVT was significantly more effective than the OPG in terms of measurement as well as the position of the mandibular canal [26].

However, Bartling [27] et al stated that the incidence of sensory dysfunction of the IAN for patients with dental implant placement was not significant if there was detailed and proper pre-operative planning to minimize the injury risk to the IAN. His study demonstrated that 405 implants were placed in 94 patients with no reports of hyperaesthesia or dysaesthesia.

Another cause of injury to the IAN is that displacement of an implant may occur due to the internal osseous architecture of the posterior body of the mandible. Additionally, the disparity in the cancellous bone structure is significant between the anterior and posterior mandible. In the posterior mandible, cancellous bone is more abundant, but less dense than in the anterior mandible [28, 29]. Schwarz et al [30] reported that the low cancellous density of the posterior mandible was greater than that of the anterior mandible. In some cases, if bone density is quite low the trephine drill may drop into spaces during preparation and lead to the displacement of the implant deeper into the mandible than planned. Penetration of the cortex should be performed for such cases where the lack of medullary bone density is visualized [28]. Pre-implant placement planning should involve the understanding of the mechanical competence of trabecular bone because bone quality and implant success has a dual correlation. Micro CT can analyze the quality as well as quantity of trabecular bone for the prognosis of implant placement [29].

Consequently, in order to diminish the possibility of a damaged IAN, pre-surgical planning combined with CT images should be used to properly visualize the relationship between the IAN and the surrounding structures in the three-dimensional space.

1.3. The mandibular canal associated with the alveolar ridge of the mandible

According to Ulm et al [31], the alveolar ridge resorption of the mandible is dependent upon the different locations. The distance from the mandibular canal to the external border of both lingual and buccal aspects does not change in any stage of the atrophying process. The location and course of the mandibular canal might alter in the atrophying process. Furthermore, it is important to note that the distance between the mandibular canal and the alveolar ridge is more likely to change than that of the distance between the mandibular canal and the inferior border of the mandible.

Levine et al [32] reported that, on average, in dentate patients, the distance from the buccal rim of the mandibular canal to the buccal margin of the mandible is 4.9 mm and the distance from the superior border of the IAN canal to the alveolar crest at the first molar is 17.4 mm.

1.4. The bifid mandibular canal

In dental literature, case reports describing bifid IAN are not common. In 1968, Patterson reported that a patient, a 30-year old white woman, had a bifid IAN with two distinct canals and two separate mental foramina at the terminal. It was seen on both the panoramic and lateral radiographs [33].

In the survey of 3612 panoramic radiographs the occurrence rate of bifid mandibular canals was 0.9% [33]. In another study, Claeys found the rate was 0.08% [8]. Langlais et al found 0.95% of cases of bifid mandibular canals, of which 33% occurred in males [34]. Either bilateral or unilateral bifid alveolar canals can occur. In terms of the dental clinic, a double mandibular canal could lead to failure in an attempt to block the IAN for anaesthesia [35, 36].

1.5. The enlarged mandibular canal

Reports of enlargement of the mandibular canal are also quite rare. Only a few cases were reported with causes usually involving lesions such as malformation or tumors. Oral pathologies associated with enlargement of the mandibular canal in most cases are as follows: neurofibromatosis, arteriovenous malformation, multiple endocrine neoplasia, and diffuse small cell lymphoma [37-40].

A clinical case was reported by Yamada in 2000 [37] in which enlargement of the mandibular canal was caused by a malignant lymphoma, but did not lead to sensory dysfunction of the IAN. The patient was a 59 year-old female who initially complained of a painless swollen lesion in the hard palate. Another lesion, 20mm in length, was detected along the right floor of the patient's mouth. The right mandibular canal was enlarged to approximately 15 mm in width, and visualized on the panoramic radiograph. On the CT, an axial image revealed this to be a homogeneous soft tissue lesion oval in shape and with a clear border.

Mojaver et al reported a case of a 38-year-old female who suffered paraesthesia of the tongue on the left side [41]. The enlarged mandibular canal was shown on both

panoramic and CT images. However, the patient had no sensory disturbance of the IAN. The relevant cause was found to be a lymphoma present in the left premolar region. Histopathological examination showed it to be a B-cell lymphoma. In the mandibular region, lymphoma is likely to relate to the inferior alveolar canal, but usually without changing the bone structure in terms of radiology [42]. Barclay reported a case of a patient with an enlarged IAN which was initially visualized on a panoramic radiograph requested for a patient who was suffering from a painful dry socket following the extraction of the left lower second premolar [43].

It was concluded that an enlarged mandibular canal was most rare and perhaps involved neoplastic lesions, whether sensory dysfunction of the IAN was relevant or not.

2. Placing dental implants at the region of the mandibular molars

Dental implants, one of the advanced techniques in terms of oral rehabilitation, have been widely used and become the choice in the treatment of replacing missing teeth. It is essential that in placing an implant, cortical bone should be involved with an angle where the forces are as perpendicular as possible [5]. Further, selection of an implant should be based not only on the appropriate size and inclination of the implant in both bucco-lingual and mesio-distal directions but also on the anatomical knowledge of the relevant area with three-dimensional visualization. A pre-surgical evaluation of the density of cancellous bone and the thickness of the cortical bone can predict the success of implant placing [44, 45].

There are many associated elements required for the successful outcome in implant placement.

- The diameter and length of an implant should depend on the site and structure where the implant is to be placed [46].
- An appropriate positioning of the dental implant placement relating to the prosthetic axis is essential [47-50].
- A pre-surgical radiograph is crucial prior to implant placement.

Today CBVT, combined with appropriate software, provides an accurate detailed image with sub-millimeter spatial resolution for dental clinicians. CBVT should be suggested to better visualize in three-dimensions the relative structures such as the location of the mandibular canal, the thickness of cortical bone and density of the medullary bone. In particular, an image of the bucco-lingual direction of the bone width, along with the use of radiopaque-marker stents is one technique to produce successful implantation [51]. Furthermore, Gaggl et al [52] reported that an exact value could be achievable within 0.14 mm when drilling close to the mandibular canal. However, he suggested that a minimum safety distance for drilling navigation was 0.3 mm. CBVT images can be used for implant planning with linear deviation at the apical tip of 2.4 mm [45]. Finally, the skill, knowledge and experience of surgeons are other factors which contribute to a successful surgical process [53, 54].

In addition to the use of CBVT and surgical navigation systems, in extremely difficult cases, the knowledge and skill of experienced surgeons is a key factor to determine the success of implant placement. Jensen et al [55] reported a successful case

where implants were placed in the severely atrophied mandible based on the technique of repositioning the IAN (Fig.1a, b). The result was excellent and performed 20 years ago.

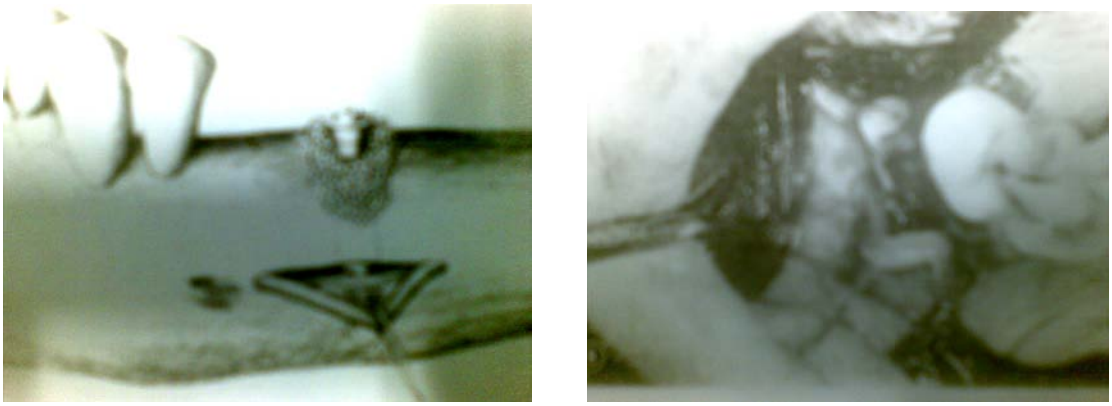

A B

Figure 1. The inferior alveolar nerve can be repositioned in the case of severe atrophy of the mandible.

(Courtesy Dr. O. Jensen 1987) [55].

3. Panoramic radiograph system and the mandibular canal

Panoramic radiography is one of the most common radiographic techniques for dental implantology. A panoramic radiograph is used as primary imaging to provide information for the assessment of implant placement planning [56]. Furthermore, clinical studies have utilized panoramic films to assess the quality and quantity of bone level. Resolution of panoramic radiographs might be lower than that of intra-oral films because film-based panoramic images utilize screens, leading to the decreased ability to detect small changes in bone surrounding the implants. Also, all panoramic films are magnified approximately 30% when the patient is ideally positioned [56]. Potter et al reported that the panoramic imaging magnification could be 40 % or 50%, depending on the system

used [47]. Thus, information from panoramic tomography may not be completely accurate.

Panoramic radiography has become an important diagnostic tool in daily clinical practice. A choice of both conventional and digital systems is available [57]. There is, however, a lack of information in the bucco-lingual direction as both systems offer only two- dimensional images. Patient positioning is crucial. Incorrect patient positioning can lead to magnification and distortion of images. In some cases, it is evident that using panoramic radiography on its own is quite adequate to visualize the mandibular canal. However, in the compromised jawbone, this technique may be insufficient. It is important to note that a surgeon works in a three-dimensional visible field, while the panoramic radiograph provides information of relevant anatomic structures in a two-dimensional mode. Jacobs stated that three-dimensional information may become necessary as risks and doubts about treatment outcome are raised [57]. Frei et al showed that the vertical magnification in panoramic radiographs was very constant pre – and post-operatively with ratio 1: 1 [58]. In general, a panoramic radiograph is still a valuable image for daily clinical application and the primary image for evaluation of pre-surgical procedures.

On a panoramic radiograph, radiological markers show the proximity of tooth roots to the IAN as follows [59]:

Root related	Canal related
Darkening	Diversion
Narrowing	Narrowing
Deflection	Loss of lamina dura
Bifid apex	

In a prospective study using panoramic radiography to predict the IAN damage following removal of mandibular third molar teeth, Smith et al reported that panoramic radiography provides the optimal methods of predicting nerve damage [59]. He argued that cross-sectional images of a CT scan are the only visual way to evaluate the level of accuracy of the relationship of the tooth root to the IAN. However, radiation dosage and cost should be considered because the outcome of the IAN deficit is not only dependent upon the relationship of the IAN to the tooth root but also poor surgical techniques or the use of neurotoxic materials which could damage the IAN, even if it is distant from the tooth root.

4. MRI and the mandibular canal

A cross-sectional image of the CT is valuable for an evaluation of the mandibular canal and to give excellent visualization of hard tissue structures [58]. In comparison, MRI clearly shows soft-tissue contrast so that the IANB can be visualized on cross-sectional and panoramic reformations. At present, few studies have been carried out associated with the course of the mandibular canal using MRI. A previous study reported by Nasel et al showed that the correlation among the MRI, CT and direct osteometry was not significantly different when the IAN was evaluated by measurement on cross-sectional images [2].

MRI has some advantages when compared with the CT and CBVT such as soft tissue detail, low level of artifact images, and especially the absence of ionizing radiation. For a pre-implant evaluation in relation to the mandibular canal, Gray et al suggested that “the use of T1-weighted sequences is indicated and the inferior alveolar nerve

bundle was identified as discrete dark structures within the bright cancellous bone" [60]. In another study, Gray et al also used the MRI to assess pre-surgical dental implant planning for appropriate sites prior to implant placement for twelve patients. The outcome was good in all patients with an assessment of a series of images in the sagittal, coronal and axial planes [61].

On the other hand, MRI has a few drawbacks. Firstly, spatial distortions of the MRI may be larger than those of the CT. Secondly, the limit of spatial resolution of the MRI is that single bone trabeculae in the transition zone cannot be clearly differentiated [2]. Finally, scan time is quite long. It can be up to 30 minutes that can cause difficulties for claustrophobic patients.

In conclusion, due to the correlation between implants and the neurovascular bundle, safety and accuracy in planning dental implant placement is essential. The above mentioned advantages can compensate for its disadvantages. MRI should be indicated for the assessment of pre-implant procedures [61] when CBVT is not available.

5. Medical CT and CBVT

5.1. The path leading to the Nobel Prize for Medicine

In 1979, The Nobel Prize for Medicine was awarded to two persons. One of these, known as the father of CT, was Godfrey N. Hounsfield who invented the first CT scanner in 1967 while working as a researcher at The Medical Systems Department of Central Research Laboratories EMI London, England [62]. The other was Allan M. Cormack, a

physics lecturer in the Physics Department, Tufts University, Medford, Massachusetts, USA [63].

In the early experiments at the laboratory, the first image was scanned from a CT unit (Fig 3). It took about 9 days to obtain the first CT image. From then on, the time of scanning each image was markedly reduced to one day, then 9 hours, 2.5 hours, 18 seconds and then 3 seconds. Currently, it takes only a few seconds to be able to capture hundreds of slices.

Cormack built up the theory that contributed an important part in the invention of the CT. He demonstrated that the theory was based on a mathematical formula as shown in Figure 2.

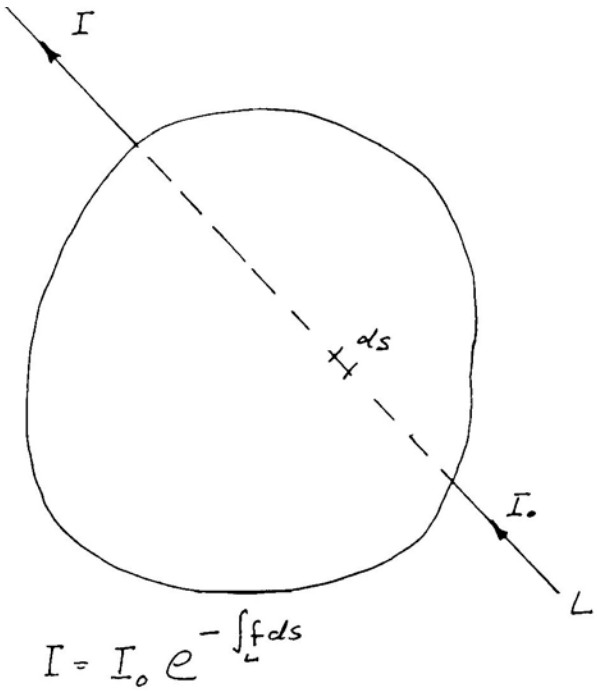

Figure 2. A mathematical formula showing the attenuation of x-rays in heterogeneous materials

He stated that “If a fine beam of gamma-rays of intensity $I_{0,}$ is incident on the body and the emerging intensity is I, then the measurable quantity $g = Ln(I_0/ I) = \int_L fds$, where f is the variable absorption coefficient along the line L. Hence, if f is a function in two dimensions, and g is known for all lines intersecting the body, the question is ‘Can f be determined if g is known?’ ”[63].

As a result, successful experiments of the two researchers created a breakthrough in the development of medical diagnostic radiography. The Nobel Prize of Medicine was awarded in great appreciation of their dedication.

5.2. The earlier CT systems

Computed Tomography also known as Computed Axial Tomography (CAT), tomography is derived from the Greek in which “tomo” means “slice” or “section” and “graphia” means “describing”.

According to Hounsfield, there were three different systems of CT scanners developed to capture images [62]. The first generation of CT scanners, known as the “translate-rotate” or “pencil-beam” system, was introduced in 1972, translating across the body, each detector taking parallel sets of readings (Fig 5). At the same time, it also rotated around the body. It had approximately 30 detectors and took 18 seconds to obtain an image.

The first generation CT scanners were designed to scan the head only. In 1972, CT was used successfully to diagnosis a brain lesion (Fig 4). Since then, many more patients have been scanned to prove that CT can distinguish the difference between normal and diseased tissues.

The second generation of this system, introduced in 1975, was designed to capture images in the form of a fan-beam. It did not translate across the body but rotated around it (Fig 6). It used around 300-500 detectors with the fan-beam and could take an image in approximately 3 seconds. It was also indicated for scanning the head region.

Finally, the third generation CT scanners appeared in 1976. The detectors were assembled in a fixed circle and only the x-ray tube swept around the patient, while the detector stayed stationary (Fig 7). Slices were taken using a fan- beam, having 700 to 1000 detectors and the exposure time was significantly reduced to only 3 seconds to take an image

Figure 3. The first image at the laboratory . (Courtesy of Dr. Hounsfield N. G. [62]).

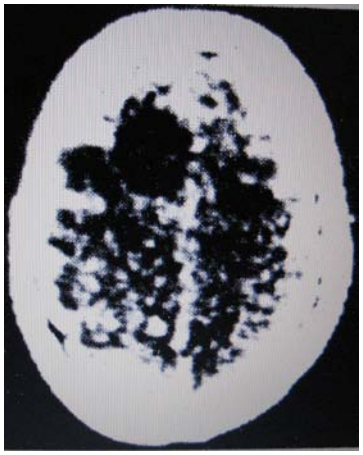

Figure 4. The first clinical image scanned from the prototype machine.

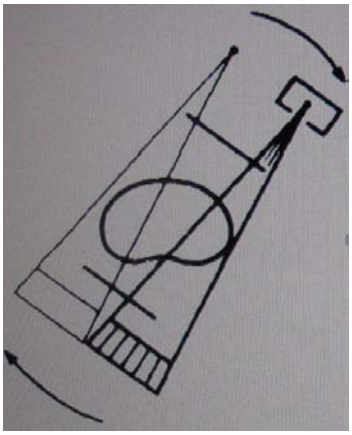

Figure 5. Translate-rotate
Scan time 18 seconds

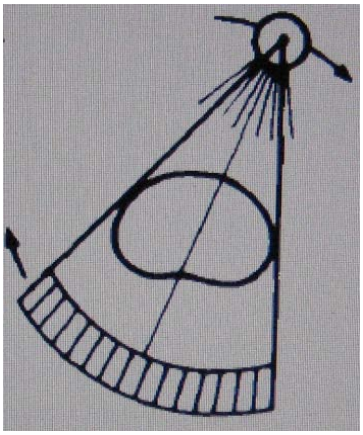

Figure 6. Rotate only
Scan time 2-4 seconds

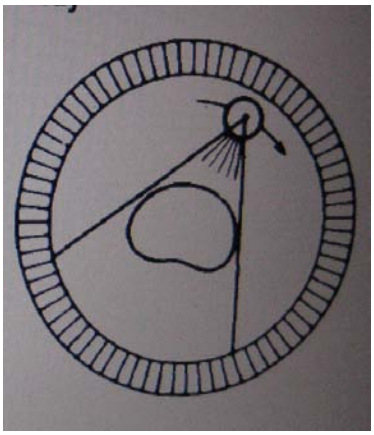

Figure 7. Stationary circular
Scan time 2-4 seconds

(Courtesy Dr. G. N. Hounsfield [62]).

Hounsfield concluded that "Computed tomography is possible to measure accurately the extent of x-rays transmission through an object and numerically transform that information into a density scale" [62].

5.3. *Contemporary CT systems*

In the early 1990s, with new designs, CT operated with multirow detectors (64 rows) and spiral scanning. Multirow scanning operated for the acquisition of several cross-sectional slices at the same time, leading to minimal scanning times [5]. In addition, state-of-the-art CT scanners were designed with 16 rows of detectors. Spiral (helical) CT included a large, arc-shaped detector, moving with a rotating x-ray tube. Furthermore, spiral CT had benefits such as reduced scanning time, improved accuracy, superior lesion detection and optimal three-dimensional reconstruction. Resolution of conventional CT is lower than that of CBVT. For example, the minimum resolution of State-of-the-art conventional CT is approximately 0.3 mm [68].

Its operating principle is that patients are moved through the machine simultaneously with the rotation of the x-ray source [57].

On the other hand, conventional CT has become popular and widely used by dental clinicians because it can eliminate some limitations of conventional radiographs. In the first place, with conventional radiographs it is impossible to view anatomical structures in three-dimensions. CT, with three-dimensional images, is more reliable for dental implant planning when compared with two-dimensional images of panoramic radiographs [44]. Secondly, conventional radiographs cannot differentiate between different soft tissues. For example, it is impossible to show structures of salivary glands on conventional radiographs. These may be visualized using sialography. Finally, the measurement density of different tissues cannot be measured when using conventional radiographs. In contrast, computed tomography can measure the attenuation of x-ray beams passing through sections where radiographs are captured from different angles. With the assistance of computed software, programs can be utilized to reconstruct radiographs from the raw data.

Although the conventional CT has some benefits in dental practice, it also has a few disadvantages such as high-radiation dose, low spatial resolution in the axial direction, high cost, and metal scatter artifacts of restorations [5]. However, Conventional CT is still the best choice for three-dimensional imaging in dentistry for places where CBVT systems are not available even though it has a few disadvantages. For example, in 2006 at the time of the commencement of this study, the CBVT system was not available in Vietnam and CT was still the best indication for three-dimensional imaging when placing dental implants.

5.4. A brief history of the CBVT system

CBVT scanners have been developed over the past two decades. Originally, CBVT was produced for angiography at the Mayo clinic in 1982 [64-66]. It was developed based on either the gantry of a conventional CT or a bi-planar C-arm system. Since then, development has continued using an image intensifier of a charge-coupled device (CCD) chain and a flat-panel detector [5]. Shinoda et al [67] reported that one CBVT unit was developed in Japan in 1997, named Ortho-CT as previously reported by Arai [68]. In this research, using a Scanora machine (Sorodex, Finland), an x-ray image intensifier of 10 cm in diameter was used to replace the film. Using a FOV that was quite small being 32 mm in height and 38 mm in diameter and the voxel size was 0.136 mm^3. Single scan of 360^0 was performed to collect 512 sets of projection data. Time for image reconstruction was 10 minutes [68].

In 1996, the first NewTom (Imago9000) was installed in Germany and Italy under the name Maxiscan. The inventors of the NewTom were the physicists Attilio Tacconi and Prof. Piero Mozzo. The first model had the same external dimension as current ones but the technology was considerably different. It used an acquisition matrix of 512x512 pixels with an 8 bit grey scale. Scan time was 75 seconds. Reconstruction time was equal to two days.

In 2001, the NewTom 9000 officially used for dental clinical applications. Now, NewTom3G 12-bit has an acquisition matrix with 1000x1000 pixels and a scan time of 36 seconds. Many CBVT systems have since been launched into the dental market. Examples of current systems include CB MercuRay (Hitachi Medical Corp, Japan), 3D

Accu-I-Tomo (J. Morita Manufacturing, Japan), i-CAT (Xoran Technologies, USA), ProMax 3D (Planmeca, Finland), 3D X-ray CT Scanner Alphard Series (Asahi, Japan), NewTom 3G and VG (RQ Verona, Italia), Picasso (E-woo Technology, Korea), PreXion 3D (TeraRecon, USA), and Scanora 3D (Soredex, Finland). In addition, some digital panoramic radiographic systems include CBVT technology [97].

5.5. Principles of Medical CT and CBVT

5.5.1. Principles of Medical CT

The operative principle of the conventional CT is illustrated in Figure 8a. Its structure consists of two components, an X-ray source and a detector mounted on a rotating gantry [5, 69].

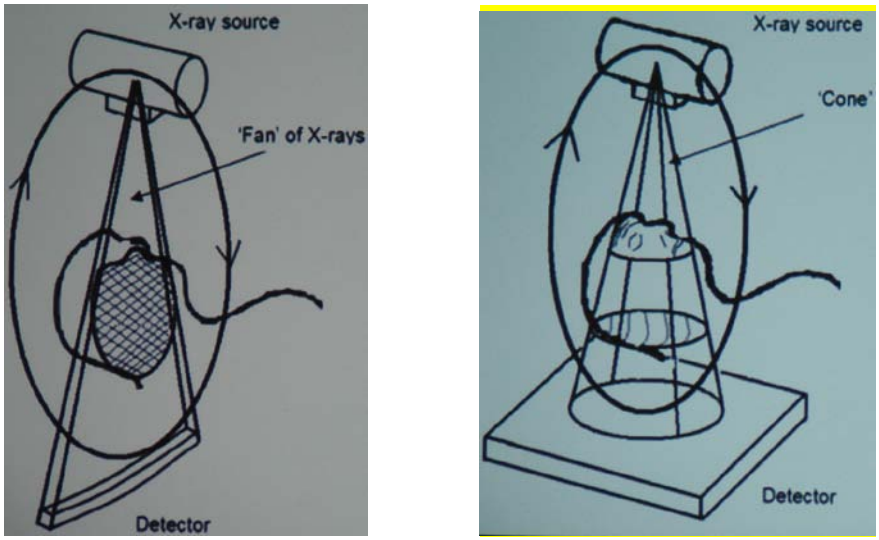

a b

Figure 8. Principles of fan-beam CT (a) and CBVT (b);

(Courtesy Prof. W. C. Scarfe, Co-Director of Radiology, Faculty of Dentistry, University of Louisville, Kentucky, USA. Lecturing at a Continuing Education Course, Faculty of Dentistry, the University of Sydney, August 2007).

Conventional CT scanners scan multiple slices that are then stacked together to obtain a final image. For this, the fan-beam CT will reconstruct an object, using slice-by-slice and then stack the slices together to create a three-dimensional representation of that object. Each single slice is obtained with a separate scan and reconstructed accordingly.

5.5.2. Principles of CBVT

CBVT with a two-dimensional detector captures whole structure of interest region by operating a 360^0 single rotation of the gantry (Fig 8b).Therefore, the time to acquire a single cone-beam projection is similar to that required by a single fan-beam projection. However, the fan- beam CT needs several scans to complete the image of an object. For this reason, the acquisition time of the fan beam is longer than that of the cone beam.

5.6. Advantages and disadvantages of CBVT

Advantages of CBVT

In the dental practice, CBVT has provided a breakthrough in imaging because it eliminates many disadvantages of conventional CT.

CBVT has existed for over two decades but its functions have not yet been fully utilized. Recently, its use has become popular in clinical dentistry because of its advantages such as

- Low radiation dose
- Image accuracy
- Reasonable cost
- Compact design

Additionally, other factors in both technologic and clinical applications as listed below have rapidly enhanced the use of CBVT in dental practice [5].

- An advanced quality flat-panel detector has been developed.
- Images have been reconstructed from raw data using powerful computers with advanced software.
- Focusing only on the dento-maxillofacial area, a sub-second gantry rotation used in medical imaging has been removed.
- Radiation dosage of CBVT is remarkably reduced when compared with conventional CT (pages 32, 33).

CBVT has been applied in dental implant planning, oral surgery, orthodontics and radiotherapy [5, 69, 70]. With the aid of appropriate software, it can use 3D cephalometrics for orthodontic assessment [70].

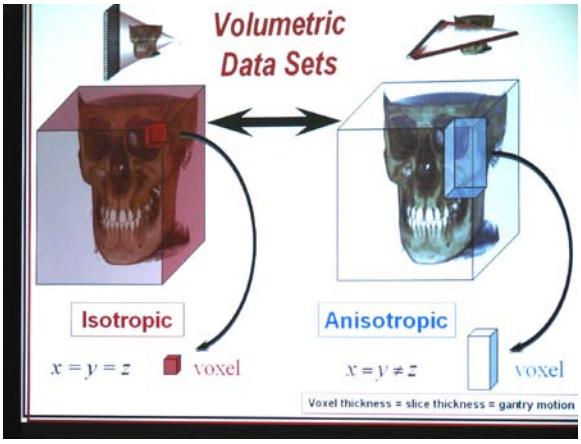

Figure 9. A isotropic voxel in CBVT is different from an anisotropic voxel in conventional CT.

(Courtesy Prof. W. C. Scarfe, Co- Director of Radiology, Faculty of Dentistry, University of Louisville, Kentucky, USA. Lecturing at a Continuing Education Course, Faculty of Dentistry, the University of Sydney, August 2007).

In digital imaging, the image quality is determined by the image resolution that is dependent upon the size of the voxels. For CBVT, voxels are structured isotropically equally in three dimensions, providing images with highly contrasted structures (Fig 9). In conventional CT, voxels are anisotropic in that the axial slice thickness is the longest dimension of voxel and is determined by slice pitch [69]. According to Rafferty [71] “the spatial resolution and image noise was considered as a function of the voxel size in 3D image reconstructions. Spatial resolution was characterized in terms of the full width at half-maximum measured in the point-spread function in an axial image of an object. Noise was characterized in the terms of the coefficient of variation (ratio of noise-to-signal) in 3D reconstructions”.

Moreover, 3D volumetric imaging of CBVT makes precise localization possible. Walker et al reported [72] that the spatial relationships of the impacted teeth relative to adjacent structures were assessed with 3D visualization software. 3D volumetric imaging of impacted teeth can show teeth presence, size of follicles, inclination of the tooth, teeth positions in the bucco-lingual direction, bone quantity surrounding the tooth, adjacent teeth, adjacent lesions, and relevant anatomical structures. Unlike with conventional modalities, CBVT can be used to evaluate tooth dimensions and angulations with no distortion [70]. Thus, it is clear that 3D imaging is an advanced tool in the management of impacted teeth.

Further, CBVT provides a sub-millimeter spatial resolution to depict important structures in detail to meet the need of clinical practice such as placing implants and

removing impacted molars [69, 73]. For example, 3D Accu-I-Tomo has a spatial resolution of two-line pairs/mm and a voxel size of 0.125 mm [67, 68].

In addition, distance measurement is easily performed at any site using an appropriate software scale tool.

Tantanapornkul et al [74] reported that in predicting the exposure of the IANB before extracting impacted third molars, the CBVT was significantly superior to panoramic images. The sensitivity and specificity of the two modalities in predicting neurovascular bundle exposure at extraction were calculated and compared. As a result, sensitivity is shown to be 93% for CBVT and 70% for panoramic images. Similarly, specificity is 77% and 63% for CBVT and panoramic images, respectively.

In conclusion, CBVT is significantly valuable due to its applications in the dental practice.

Disadvantages of CBVT

There are a few disadvantages of CBVT.

- Image noise reduces the clarity of an image.
- CBVT cannot display soft tissue contrast.
- CBVT images have metal scatter artifacts in the same way as medical CT.
- The cost of CBVT should be considered when setting up this system in developing countries such as Vietnam where CBVT, at the time of the study, is not yet available. At present, in Vietnam, implant placement is performed using a

panoramic radiograph and /or CT images and relies mainly on experienced clinicians.

5.7. Flat-panel detector and intensifier detector

Principles of flat panel detector and the image intensifier are different as shown in Fig 10.

5.7.1. Flat panel detector

The flat panel detector consists of a CsI scintillation screen and a photo-sensor array (Fig 10a). The photo-sensor array consists of arrayed photodiodes and switching devices. The function of a scintillator is to convert the x-ray beam into an optical signal, which is then converted, to the electrical signal by the photodiode. This electrical signal is, in turn, read by the switching device array [75]. The flat panel detector has some advantages. Its image has veiling glare or no distortion. Further, its detector pitch is usually smaller than that of the intensifier detector [76-78].

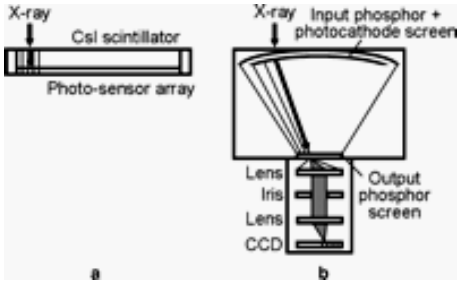

Figure 10. Components of the detectors: (a) flat panel detector and b) image intensifier detector (Courtesy Dr. R. Baba [75]).

5.7.2. Intensifier detector

The image intensifier detector consists of an x-ray image intensifier, optics and a CCD television camera (Fig 10b). The x-ray beam is converted to the optical signal by

the input phosphor screen. This optical signal is then transformed to electrons by the photocathode screen. Electrons are accelerated by the electrical field inside the image intensifier and converted back to the optical signal at the output phosphor screen. The intensity of the optical signal is adjusted by an optical iris and the signal is then detected by the CCD. The read-out image includes geometrical distortion and a blurring component of veiling glare generated by the image intensifier [75].

As described above, the flat panel detector is unlike the image intensifier detector in that it does not have an optical iris as the direct means for adjustment. Baba quoted; "This makes it difficult to prevent saturation of the pixels. Correction for saturated pixels, defective pixels, and the sensitivity of the detector is applied in the new system and reduces streak and ring artifacts in reconstructed images" [75]. For this, the image quality of CBVT has improved due to the use a flat-panel detector system.

5.8. Transmitted Intensity and Linear Attenuation Coefficient

5.8.1. Transmitted Intensity

The change of x-ray beam intensity at a certain distance in the material is described in the form of an equation as follows:

$$dI(x) = - I_0(x).n.\sigma.dx$$

Where dI : the change in intensity

I_0 : the initial intensity

n : the number of atoms/ cm^3

σ : a proportionate constant that reflects the total probability of a photon being scatted or absorbed

dx : the incremental thickness of material traveled

When this equation is integrated, it becomes

$$I = I_0 e^{-n\sigma x}$$

The number of atoms/cm^3 (n) and the proportionate constant (σ) are usually combined to yield the linear attenuation coefficient (μ). Therefore, the equation becomes:

$$I = I_0 e^{-\mu x}$$

Where I : the intensity of photons transmitted across some distance

I_0 : the initial intensity of photons

μ : the linear attenuation coefficient

x : distance traveled

5.8.2. The Linear Attenuation Coefficient (μ)

The linear attenuation coefficient (μ) describes the fraction of a beam of x-rays that is absorbed or scattered per unit thickness of the absorber. This value accounts for the number of atoms in a cubic cm volume of material and the probability of a photon being scattered or absorbed from the nucleus or an electron of one of these atoms.

5.9. Noise and signal in digital imaging

Noise is known as an unwanted signal. Signal-to-noise ratio (SNR or S/N) is defined as the ratio of a signal power to the noise power corrupting the signal. It is clear that signal-to-noise compares the level of a desired signal to the level of background noise. The higher the ratio the less obtrusive the background noise is.

The signal-to-noise ratio is:

$$SNR = \frac{N}{\sqrt{N}} = \sqrt{N}$$

Where N : the average number of photons collected.

When N is very large, the signal-to-noise ratio is also very large. It seems that photon noise has more significance when the number of photons collected is small.

Image quality of a CBVT scanner can be affected by noise and poor focus, leading to an image that can be stray noise and with a blurred appearance. Normally, poor focus has the effect of a Gaussian blur which affects the clarity of the image. A technique that could mitigate noise and de-blur an image would be very desirable since it would improve the quality of digital images. Baba reported that with equal detector pitches, reconstructed images of the flat panel detector have less noise than those of the image intensifier detector [75].

6. Application software associated with CBVT

Previously, some systems of computed-aided navigation were used for dental implant placement [79, 80]. With an accuracy of less than 1 mm positioning errors, the optical tracking system was reliable in the dental practice, but it was hard to control during the surgical procedure due to the difference in size between the camera and Light Emitting Diode (LED) on the surgical tool [81].

At present, there is much software available to aid interaction with the CBVT in dental clinical practice especially pre-surgical and pre-implant treatment planning such as Simplant, Procera, and Amira etc. Reconstruction of CBVT images are exported to

DICOM (Digital Imaging and Communications in Medicine) format and then imported to appropriate software. This software also allows users to make measurements on the 3D model, permitting an accurate measurement of a surgical site in the three-dimensional space in relation to the mandibular canal. When radiographic images are available, interactive computer software imaging can transfer information to evaluate and plan for implant treatment placement [82].

Wanschitz et al [83] reported that the optimal positioning of an implant could improve biomechanical, functional, aesthetic and phonetic results. When the implant has been accurately placed both the biomechanical and aesthetic requirements of the jaw are achieved. A substantial improvement could only be achieved with a higher CT-scan resolution. It was concluded that computer-aided software for pre-surgical treatment planning can reach a feasible level of accuracy in dental clinical practice.

7. Radiation Dose

Table 1 shows an effective dose (E) among other modalities. In CBVT units, fields of view (FOV) can be selected to reduce the size of the collimation of the primary x-ray beam to the area of interest. This minimizes the radiation dose for the patient. The FOV of each CBVT unit may differ depending on the manufacturer. For example, the NewTom3G unit consists of three fields of view, 12", 9", and 6". The i-CAT unit is designed with two fields of view, 13 cm x 16 cm and 16 cm x 22 cm. Additionally; CBVT acquires all base images in a single rotation of 360^0 so that scan time is significantly reduced (table1) when compared with conventional CT. Previous reports showed that the effective radiation dose of CBVT is only about 10 microsieverts (μSv),

which is about 1– 2% of conventional CT [67, 68]. Tuzkymaz et al [84] reported that radiation dosage of the NewTom3G scanner is approximately 12.0 µSv which is equivalent to or less than the dose required for 5 dental films using D speed film but four times greater than a panoramic tomograph, while a medical CT scanner requires a radiation dose 40-60 times greater. According to Brooks and White [122], an effective dose of i-CAT 20 second scan was 68 µSv; i-CAT 10 second scan was 34 µSv; Daily background was 8 µSv; Panoramic (Average): 10-15 µSv; Digital Panoramic was 4.7 – 14.9 µSv; Highest Film Panoramic was 26 µSv; Full mouth series were150 µSv; Medical CT was 1200-3300 µSv[122].

A dosimeter study was done on three CBVT devices, including the CB MercuRay, the NewTom 3G and the i-CAT to calculate effective dose. In this study, 24 thermoluminescent dosemeters (Landauer, Inc, Glenwood, IL) were inserted into a RANDO phantom (Nuclear Associates, Hicksville, NY). The outcome of this study showed that effective dose for standard full FOV were 44.5, 134.8, 476.6 µSv for the NewTom 3G, the i-CAT and CB MercuRay (effective dose of ICRP 1990) and 58.9, 193.4, 557.6 µSv for the NewTom 3G, the i-CAT and CB MercuRay (effective dose of ICRP 2005). Thus, when comparing with the Newtom 3G full FOV dose, the i-CAT was 1.5 times more dosage while CB MercuRay required 11 times more dosage as calculated using an effective dose of ICRP 1990 [86]. Further, it was noted that the operating parameters for the i-CAT are not adjustable by the user, while those of the NewTom 3G adjust automatically based on the patient size. For example, a small child may receive up to 40% less radiation than that of an adult for the same FOV [120, 121].

A manufacturer showed the radiation exposure to a patient from a conventional CT to be approximately 100-300 μSv for the maxilla and 200-500 μSv for the mandible. The radiation exposure for both mandible and maxilla from the i-CAT is between 34-102 μSv, depending on the time and resolution of the scan [118]. White and Pharoah stated that CBVT is less expensive than CT and the radiation dose delivered to the patient may be as little as 3% to 20% that of a conventional CT scan, depending on the equipment used and the area scanned [119].

In more recent studies of radiation dosage and image quality, Loubele et al [85] reported that the i-CAT machine had the lowest radiation dose (107 μGv mm) versus image quality when evaluating radiation dose among the 3D Accu-I-Tomo, MercuRay, and NewTom3G machine with dosages of 1569 μGv mm, 446 μGv mm, and 249 μGv mm, respectively. When doing research to evaluate absorbed and effective doses for implant planning using three units including a 3D Accuimoto, a CB MercuRay and a conventional multidetector CT (MDCT) , Okano et al [117] found that effective dose of conventional CT was almost ten times more than that of CBVT. The effective dose from 3D Accuitomo was from two to eight times higher than that from panoramic radiography, ranging from 4 to 10 μSv depending on the system used and the method employed [117]. In addition, the absorbed dose of the mandible was ranged from 2.47 to 23.52 mGy. The effective dose using the tissue weighting factors was estimated to be about 18-66 μSv, 452 μSv, and 596 μSv for 3D Accuimoto, CB MercuRay, and MDCT respectively. Tissue weighting factors were listed in table 2.

As a result, published reports indicate that the effective dose varies depending on the type and model of CBCT equipment and FOV selected [123]. It seems that the effective dose

exposing to patients is the lowest about 45 µSv from the NewTom 3G and highest of 478 µSv from the CB MercuRay, while this is about 1200 µSv from the conventional CT system [86, 117, 123].

Table 1. Comparison of effective dose (E) by tissue weighting protocol, as a multiple of panoramic images and as a percentage of annual per capital background X-ray dose [86].

Technique	E(µSv)	E (µSv)	Dose as multiple of single Panoramic dose	Dose as multiple of single Panoramic Dose	% of annual per capita background	% of annual per capita background
	ICRP 1990	ICRP 2005	ICRP 1990	ICRP 2005	ICRP 1990	ICRP 2005
NewTom 3G-12" FOV	44.5	58.9	7	4	1.2%	1.6%
i-CAT-12" FOV	68.7	104.5	11	8	1.9%	2.9%
Panoramic (Orthophos plus DS)	6.3	13.3	1	1	0.2%	0.4%
Maxillo-mandibular CT scan	2,100		336		58.3%	
Maxillary CT scan	1,400		224		38.9%	

(Courtesy Dr. B. J. Ludlow [86])

Table 2. Tissue weighting factors as defined by the International Commission on Radiation Protection (ICRP) 1990 and 2007 recommendations [117].

Tissue	Tissue weighting factor	Sum of tissue weighting factor
ICRP 1990		
Gonads	0.20	0.20
Bone marrow, colon, lung, stomach	0.12	0.48
Breast, bladder, oesophagus, liver, thyroid	0.05	0.25
Bone surface and skin	0.01	0.02
ICRP 2007		
Gonads	0.08	0.08
Bone marrow, colon, lung, stomach, breast and remainder tissues (14 in total)	0.12	0.72
Bladder, oesophagus, liver and thyroid	0.04	0.16
Bone surface, brain, salivary glands and skin	0.01	0.04

.

Table 3. Comparative radiation exposures from CBVT systems [123]

CBCT units	Technique	Radiation dose	Imaging surveys		BERT(*)	
		Effective dose (μSv)	Equivalent Panoramic	%of conventional CT	No of days	% Annual
CB MercuRay	12’’/ 9’’/ 6’’ FOV	477/289/ 169	80/ 48/ 28	22.7%/ 13.8%/ 8%	116 /70/ 41	31.8%/19.3%/ 11.2%
Galileos	Default/Maximum	29/ 54	5/ 9	1.3%/ 2.6%	7/ 13	1.9%/ 3.6%
i-CAT	12’’ FOV	135	23	6.4%	33	9%
Iluma	Low/ High	61/ 331	10/ 55	2.9%/15.8%	15/ 81	4%/ 22%
NewTom 3G	12’’ FOV	45	8	2.1%	11	3%
ProMax 3D	Small/Large	157/210	26/35	7.5%/ 10%	38/ 51	10.4%/14%

(*) BERT: Background Equivalent Radiation Time.

Chapter 2

MATERIALS AND METHODS

1. Ideas leading to this research

Four ideas led to this study. Firstly, the author was interested in CBVT so that when the Newtom3G machine was seen in operation that became the motive to study the CBVT system in depth. This system was not available in Vietnam when the author came here to study in 2006.

To find the position of the IAN prior to surgery is very important. Comparing various imaging modalities to find the one that gave the best visualization was a further motive towards this study.

In many cases, the direction of dental implants placed in the lower posterior region tends to be nearly parallel to the midline of the mandible and in the direction of the lower premolars, the mesial root of the first lower molar, and the first and second maxillary molars (Fig. 11). For this study, cross-sectional images were chosen parallel to the midline instead of perpendicular to crest of the ridge of the mandible as in previous studies.

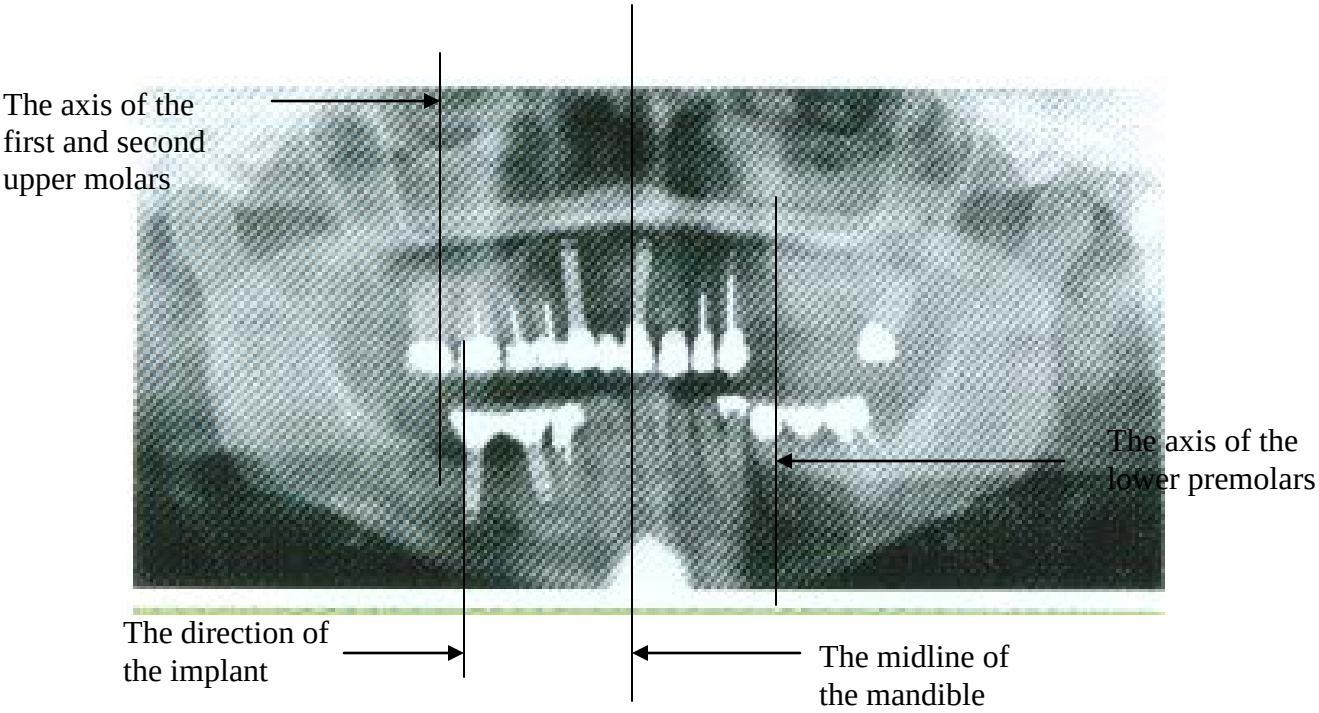

Figure 11. Direction of dental implants placed in posterior molars has the tendency to parallel to the midline of the mandible.
(Courtesy of Dr. M. Block. 2007)

In a textbook of occlusion, Mohl et al reported that the disto-mesial distance of the occlusal surface of the molars is approximately 10 mm [87]. Using this as a baseline the idea for development of the present study arose.

2. Study sample

Fourteen dry mandibles of Vietnamese adults were collected from the Department of Medical Anatomy, Medical and Pharmaceutical University of Ho Chi Minh City, Vietnam. Demographic data of the study sample were not available so that age and gender were not identified. There were two criteria involved in the selection the sample.

- All mandibular canals had to be able to be visualized on the CBVT and OPG images on the left and right sides.

- All either edentulous or dentate dry mandibles had to be bilaterally symmetrical at the region of the first, second, and third lower molars.

Four dry mandibles were discarded because they did not confirm to this criteria. Finally, ten dry mandibles were used, seven of which were completely edentulous and the remaining three were dentate bilaterally in the molar region.

3. Study design

For the present study, four Gutta Percha (GP) points, known as markers, were attached to the dry mandible on both buccal and lingual sides (Fig.12) and located in a posterior direction from the distal border of the mental foramina at intervals of 10 mms, namely, M_0, M_1, M_2 M_3. It became clear that sites M_1, M_2, M_3 lie in the region of the first, second, and third molars, respectively. From the midline of the mandible lines were drawn parallel and closely together until a position at the distal border of the mental foramen was reached (Fig.13 and 14).

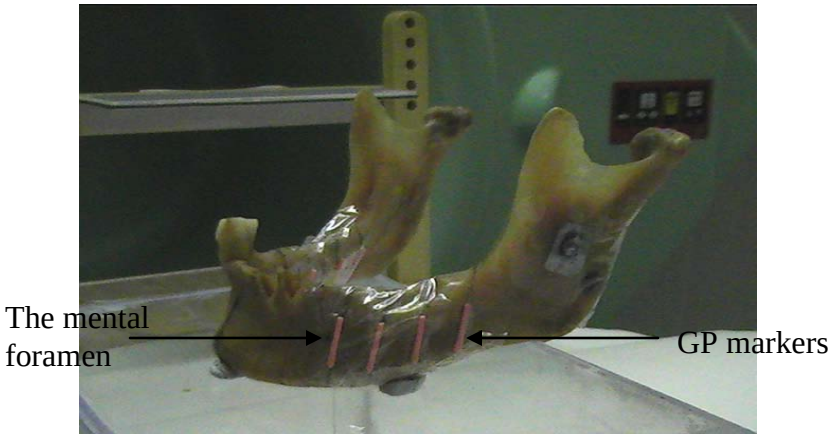

Figure 12. GP markers were attached parallel to the mandible at four sites M_0, M_1, M_2 and M_3 with intervals of 10.00 mm measured from the distal border of the mental foramina in a posterior direction.

Figure 13. The dry mandible was cut at four sites M_0, M_1, M_2 and M_3 using a hack saw.

Figure 14. Parts of the dry mandible after cutting.

4. The disto-mesial distance of the occlusal surface of the first, second, and third molars

On average, the mesiodistal dimension of mandibular molars is 11mm, 10.5mm, and 10mm for the first, second, and third molars, respectively [87]. For this reason, in the present study, four sites were marked $M_{0,}$ M_1, M_2 and M_3 by GP points that were attached from the distal border of the mental foramina in a posterior direction at intervals of 10 mm (Fig12). It is clear that positions M_1, M_2 and M_3 were located to lie in the region of the first, second, and third molars, respectively. This was also demonstrated on the three dentate dry mandibles of this study.

5. Imaging modalities

Three modalities were used to image the dry mandibles; the NewTom3G, the i-CAT, and the Orthophos panoramic machines.

6. Positioning of the dry mandibles prior to imaging

On the Newtom 3G unit, each dry mandible was fixed on a plastic box in the patient's head position and a chin rest was used to keep the dry mandible stable prior to moving it into the gantry (Fig.15). A preliminary scout view displayed on the screen of the personal computer workstation before taking the film assisted in the correct mandible positioning. This was determined, when the dry mandible was in the gantry, by the use of two lines of the laser beam (Fig.16). The vertical light was to determine the midline of the dry mandible and the horizontal light passed through the central region of the ramus

of the mandible. The latter was adjusted by moving the patient table up and down. The intersection between them was centre of the volumetric acquisition.

Similarly, on the i-CAT machine, each dry mandible was placed on the chin rest and a preliminary scout view was taken to determine a proper mandible positioning. The correct position for the mandible was then determined by adjustment of two laser lights in the vertical and horizontal directions. The image acquisition was then a single 360^0 rotation.

Finally, the dry mandibles were placed on a plastic box that was fixed on the chin rest of the Orthophos OPG machine so that they were located on the focal trough of the machine using the bite block to adjust the position of the mandibles. To simulate the soft tissue attenuation and prior to exposure a latex balloon filled with water was placed in front of the collimator of the machine.

Figure 15. Positioning of the dry mandible prior to scanning in the NewTom 3G machine.

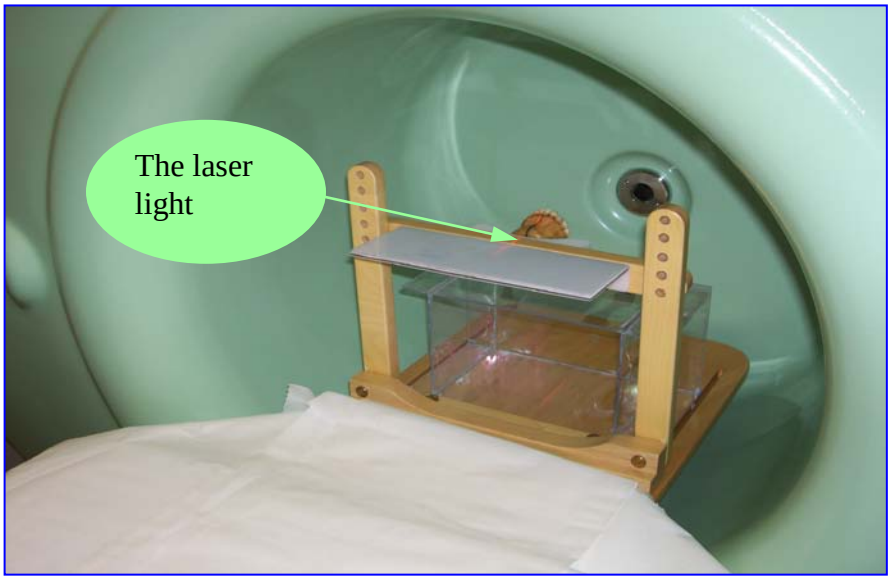

Figure 16. The dry mandible was moved into the gantry using the laser light to determine its position.

7. Measurement methods

7.1. On the Newtom3G and i-CAT

On the NewTom3G and i-CAT machines, axial images, with eight GP markers at the lingual and buccal aspects at each side of the mandible were chosen (Fig 17). A single cross-sectional tool was used to draw parallel lines through GP markers in the bucco-lingual direction at sites M_0, M_1, M_2 and M_3 respectively (Fig.17) to obtain eight cross-sectional images from each axial image (Fig.18).

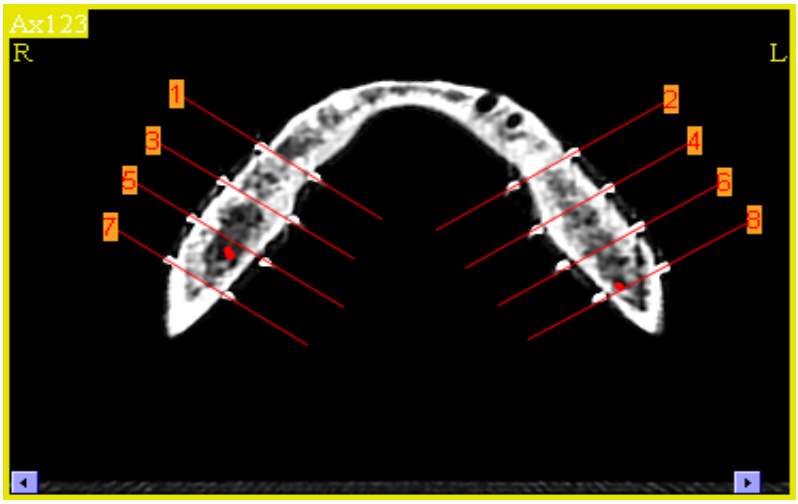

Figure 17. The cross-sectional tool was used to "cut" the axial image at eight sites on the left and right sides in the bucco-lingual direction.

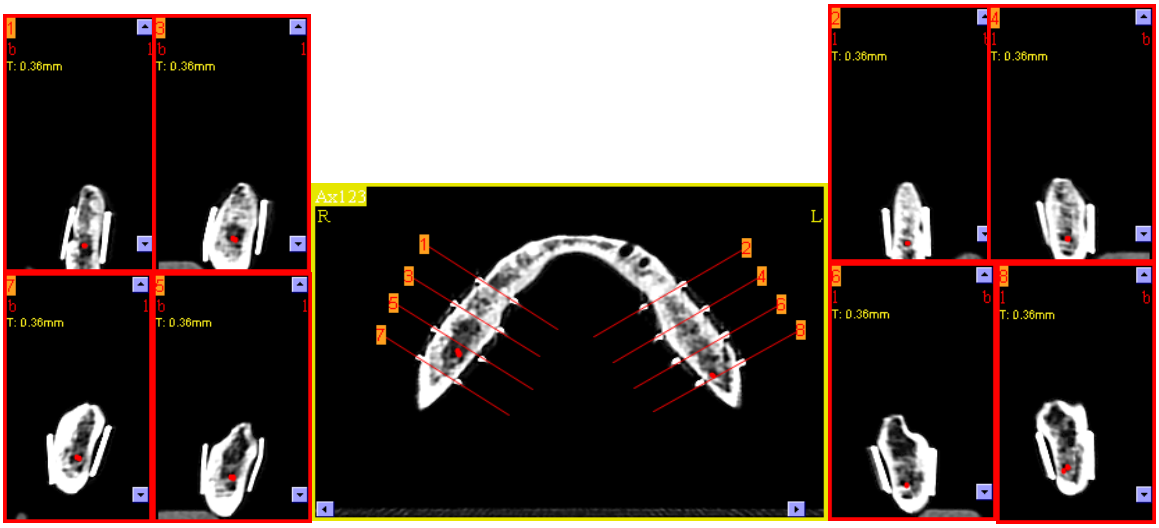

Figure 18. Eight cross-sectional images were obtained after using the cross-sectional tool to cut eight positions of the axial image

On the cross-sectional images, a series of variables at sites M_1, M_2, and M_3 were measured on the left and right sides of the mandibles. There were six distances to be

measured on each cross-section image namely AC, BC, LC, IC, and BW as shown in Figure 19. Detailed measurements of the variables were illustrated in Figure 20.

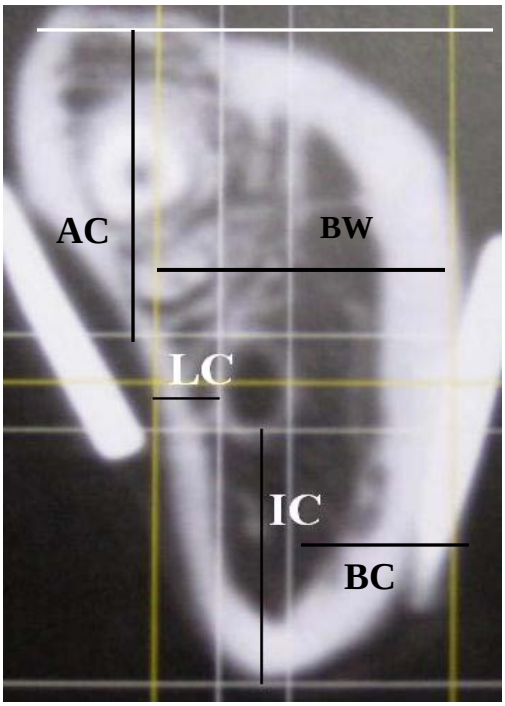

Figure 19. The distances AC, BC, LC, IC, and BW were measured on the cross-sectional image.

AC : distance from the alveolar crest of the mandible to the superior border of the mandibular canal

BC : distance measured from the buccal rim of the mandibular canal to the buccal margin of the mandible

LC : distance measured from the lingual rim of the mandibular canal to the lingual margin of the mandible

IC : distance measured from the inferior rim of the mandibular canal to the lower border of the mandible

BW: Bone Width: distance measured from the lingual margin to the buccal margin of the mandible.

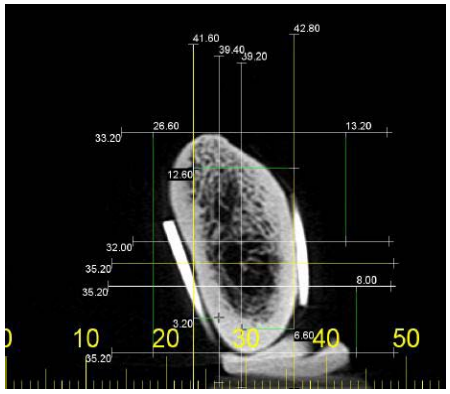

Figure 20. Detailed measurement of variables on the cross-sectional image with magnification to 180%.

7.2. On the dry mandibles

After collection of the data from both the NewTom3G and i-CAT machines was completed, the dry mandibles were sacrificed by cutting at the four marked positions M_0, M_1, M_2, and M_3. A caliper, with decimal at 0.00, was used to measure these variables from cross-sections of the dry mandibles that had been cut by a hacksaw (Figs 21-23).

Figure 21. The cross-section of the mandible after cutting showing the mandibular canal.

Figure 22. The cross-section of the mandible prepared for the measurement of the distances.

Figure 23. Measurement of the distances on the cross section of the dry mandible using the caliper.

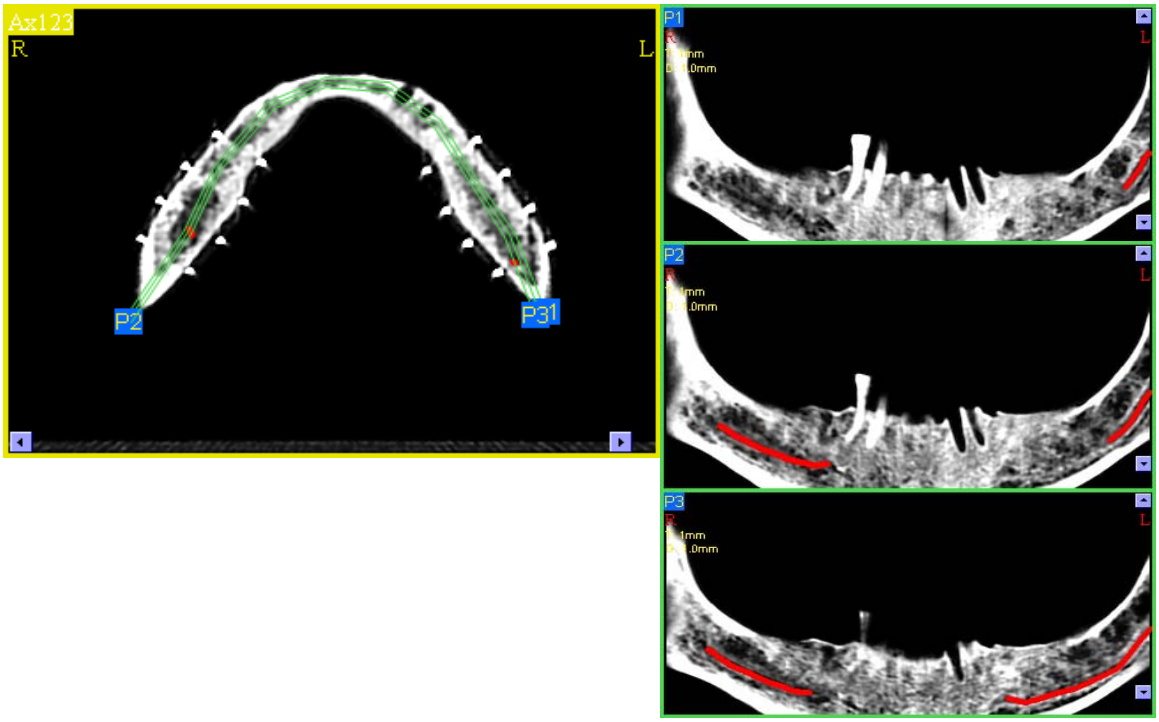

Figure 24. The cross-section of the panoramic images from the NewTom3G with slices of 1mm. A marker tool highlighted the inferior alveolar nerve.

8. The NewTom 3G Machine

The NewTom3G machine is set up in the Department of Diagnostic Imaging Sydney Dental Hospital, New South Wales, Australia (Fig 25). The NewTom3G is operated at 110 kVp and 10 mA using a high frequency generator with 0.3mm focal spot size. Images are acquired using a single 360^0 rotation including 306 basic projections and 12 bit greyscale. Images are captured in approximately 36 seconds but x-ray exposure to the patient is only for 5.4 seconds. The FOV is set up at 12", and the voxel dimension is 0.2mm. Cross-sectional images are set up to a thickness of 1mm, with a step of 0.5mm, and using a broken line. These images are recorded on a CCD-chip with a matrix of 1000 x 1000 pixels [88] as raw data and transferred through a Windows based program into axial, sagittal and coronal slices. Software QR NNT version 2.00 was used Copyright

(C) QR 2001-2004, QR srl.via Silvestrini, 20-37135-Verona, Italy [89]. Primary reconstruction of the data takes approximately 1-3 minutes and is automatically carried out immediately after acquisition. Secondary reconstruction is performed in real time and provides axial and coronal two-dimensional multi-planar reformatted slices.

At each site of $M_{0,}$ M_1, M_2 and M_3, each cross-sectional slice was selected to visualize the mandibular canal for its measurement. The axial and cross-sectional images were contrasted and magnified to 180% for convenience.

9. I- CAT machine

The i-CAT was manufactured in June 2006 by Imaging Sciences International Inc, Hatfield, PA, 19440 USA, Model No: 9140-00000000K, Serial No: ICU 07483.This unit is set up at the Oral Imaging Unit, Westmead Centre for Oral Health, Westmead Hospital, New South Wales, Australia (Fig. 26). The i-CAT machine is operated at 120 kVp and 3-8 mA using a high frequency generator with 0.5mm focal spot size. Images are acquired at a single 360^0 rotation including 306 basic projections with the exposure time of 20 seconds and 14 bit greyscale. The FOV is set up at 16 cm x 22 cm, and the voxel dimension was 0.2mm. Primary reconstruction of the data can take up to seven minutes, depending on the protocol selected and is automatically carried out immediately after acquisition. Secondary reconstruction is performed in real time and provides axial and coronal two-dimensional multi-planar reformatted slices.

At each site of $M_{0,}$ M_1, M_2 and M_3, each cross-sectional slice was selected to visualize the mandibular canal for its measurement. The axial and cross-sectional images were contrasted and magnified to 180% for convenience in measurement (Fig. 20).

The basic images of these two machines were reconstructed based upon the the Feldkamp-Davis-Kress algorithm to form the CBVT image volume [90-92].

10. Orthophos OPG machine

Panoramic images were acquired by the Orthophos (Siemens) panoramic machine (Fig. 27). On the panoramic images, IC distances at M_1, M_2, and M_3 sites were measured to assess the course of the mandibular canal on bilateral sides of the mandible (Fig. 28) as well as to compare them with the CBVT system (NewTom3G and i-CAT). The Orthophos panoramic machine is set up in the Department of Diagnostic Imaging, Sydney Dental Hospital, New South Wales, Australia.

Figure 25. The NewTom3G machine at the Sydney Dental Hospital, New South Wales, Australia

Figure 26. The i-CAT unit at the Westmead Hospital, New South Wales, Australia.

Figure 27. The Orthophos OPG machine at the Sydney Dental Hospital, New South Wales, Australia

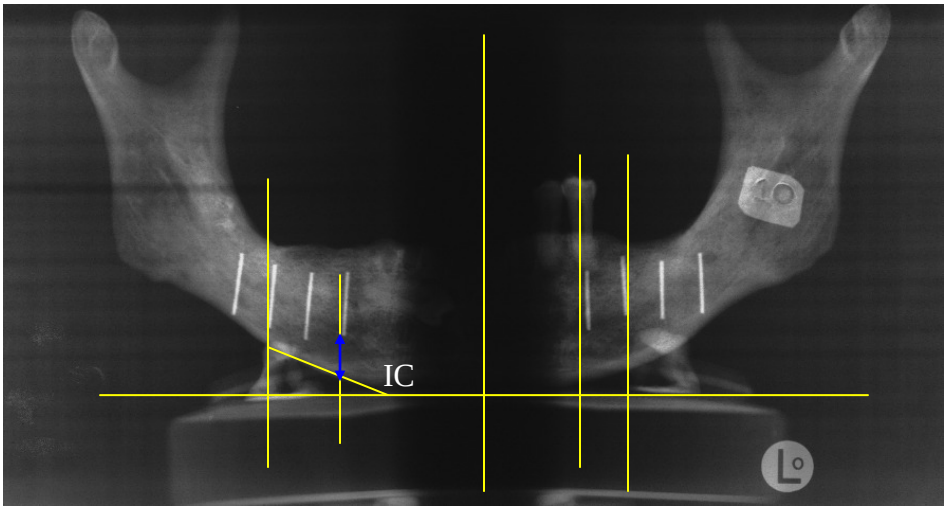

Figure 28. On the Orthophos OPG machine, IC distances are measured at sites M_1, M_2 and M_3 on both sides

11. Data analysis

Data were managed by Microsoft Office Excel 2003 and transferred to the statistics software of Statistics Package for Social Sciences (SPSS) version 15.0 for Windows for analysis. Data were presented as Mean, SD, Mean Difference and SEM with the decimal at 0.00. T-test and One-way ANOVA were used to analyse variables measured in which t-test was used to analyse variables with paired samples. One-way ANOVA was used with adjustment for multiple comparisons of Bonferroni. Statistical significance was assumed with a P-value of 0.05 or less.

Chapter 3

RESULTS

1. Results of variables measured from the NewTom3G and i-CAT units and the manual measurement using the dry mandible

1.1. At the region of the lower first molars

Table 2. Statistics of measured variables at the region of the first right mandibular molar.

Right Side	Mean±SD			P-value[(a)]
	NewTom 3G	i-CAT	Dry M	
AC	12.38±4.55	12.62±3.50	12.10±3.92	0.55
BC	6.18±0.92	6.25±0.88	6.70±0.85	0.01[*]
LC	3.71±0.80	3.62±0.95	3.55±0.83	0.72
IC	9.44±1.58	8.97±1.35	9.38±1.55	0.30

DryM : Dry Mandible
SD : Standard Deviation
AC : distance measured from the alveolar crest of the mandible to the superior border of the mandibular canal
BC : distance measured from the buccal rim of the mandibular canal to the buccal margin of the mandible
LC : distance measured from the lingual rim of the mandibular canal to the lingual margin of the mandible
IC : distance measured from the inferior rim of the mandibular canal to the lower border of the mandible
(a) : One-way ANOVA with adjustment for multiple comparisons of Bonferroni
(*) : the mean difference is significant at the 0 .05 level

Table 2 shows the group data of the four distances measured in the first lower molar area on the right side. There was no significant difference from the Newtom3G, i-CAT and manual measurement in the measurement distances including AC (F=0.62, P=0.55), LC

(F=0.19, P=0.72) and IC (F=1.28, P=0.30). AC distance in the manual measurement was slightly smaller than that in the i-CAT and NewTom3G. Furthermore, LC and IC in the NewTom3G were slightly larger than those of the i-CAT. However, these differences were not statistically significant. BC of the NewTom3G was significantly smaller than that of the manual measurement (F=8.8, P=0.01)*.

Table 3. Statistics of measured variables at the region of the left mandibular first molar .

Left Side	Mean±SD			P-value(a)
	NewTom 3G	i-CAT	DryM	
AC	13.07±3.98	13.02±3.79	13.57±2.49	0.35
BC	5.75±0.90	5.85±0.86	6.09±1.28	0.43
LC	3.23±0.75	3.22±0.78	3.34±0.90	0.83
IC	9.17±1.39	9.24±1.57	9.72±1.50	0.13

DryM : Dry Mandible
SD : Standard Deviation
AC : distance measured from the alveolar crest of the mandible to the superior border of the mandibular canal
BC : distance measured from the buccal rim of the mandibular canal to the buccal margin of the mandible
LC : distance measured from the lingual rim of the mandibular canal to the lingual margin of the mandible
IC : distance measured from the inferior rim of the mandibular canal to the lower border of the mandible
(a): : One-way ANOVA with adjustment for multiple comparisons of Bonferroni

Table 3 shows variables measured in region of the left mandibular first molar. Manual measurement showed no significant difference from Newtom3G, and i-CAT in measuring the distances AC (F=1.13, P=0.35), BC (F=0.87, P=0.43), LC (F=0.09,

P=0.83) (Fig29) and IC (F=0.26, P=0.13). Four statistical parameters of the manual measurement were slightly larger than those found in the NewTom3G and i-CAT, but these differences were not statistically significant.

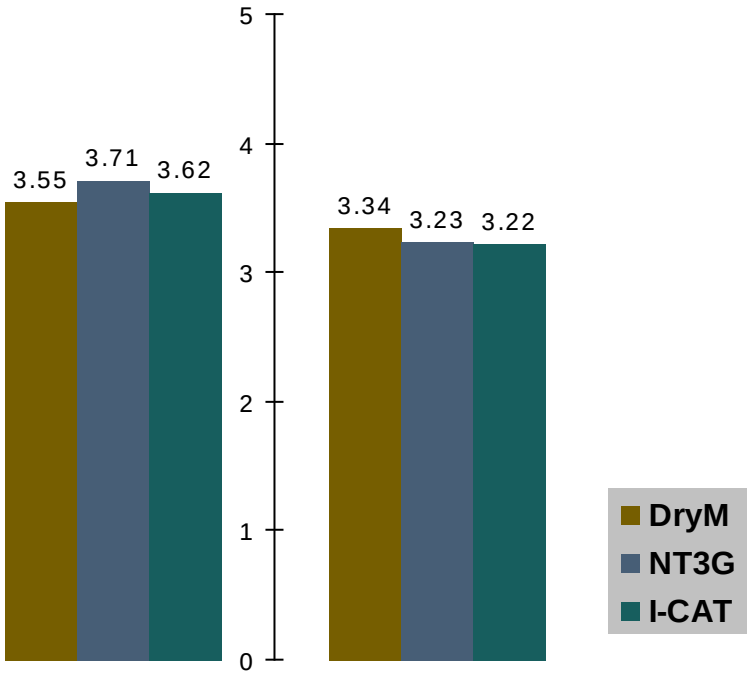

Figure 29. LC : distance measured at the region of the first molar on the right and left sides from the NewTom 3G, i-CAT and manual measurement. DryM : Dry Mandible.

1.2. At the region of the lower second molars

Table 4. Statistics of measured variables at the region of the right mandibular second molar.

Right Side	Mean±SD			P-value[(a)]
	NewTom 3G	i-CAT	DryM	
AC	11.83±5.18	11.68±2.97	11.79±3.24	0.92
BC	7.01±0.22	6.87±0.33	7.34±0.30	0.23
LC	3.66±0.97	3.66±0.87	3.48±0.84	0.36
IC	9.86±1.65	9.46±1.40	9.71±1.39	0.56

DryM : Dry Mandible
SD : Standard Deviation
AC : distance measured from the alveolar crest of the mandible to the superior border of the mandibular canal
BC : distance measured from the buccal rim of the mandibular canal to the buccal margin of the mandible
LC : distance measured from the lingual rim of the mandibular canal to the lingual margin of the mandible
IC : distance measured from the inferior rim of the mandibular canal to the lower border of the mandible
(a): : One-way ANOVA with adjustment for multiple comparisons of Bonferroni

Table 4 presents group data of the four distances measured in the region of the lower second molar on the right side. Although variables measured were either slightly smaller or larger between the NewTom3G, i-CAT and manual measurement, these differences were not statistically significant (P>0.05) with AC (F=0.02, P=0.92), BC (F=1.66, P=0.23), LC (F=, P=0.36) and IC (F=0.60, P=0.56).

Table 5. Statistics of variables measured at the region of the left mandibular second molar.

Left Side	Mean±SD			P-value[(a)]
	NewTom 3G	i-CAT	DryM	
AC	12.48±3.29	12.12±3.37	12.11±2.29	0.58
BC	6.67±0.77	6.70±0.90	6.89±1.03	0.60
LC	3.39±1.01	3.36±0.57	3.49±1.76	0.84
IC	9.37±0.37	8.83.±0.42	9.30±0.34	0.30

DryM : Dry Mandible
SD : Standard Deviation
AC : distance measured from the alveolar crest of the mandible to the superior border of the mandibular canal
BC : distance measured from the buccal rim of the mandibular canal to the buccal margin of the mandible
LC : distance measured from the lingual rim of the mandibular canal to the lingual margin of the mandible
IC : distance measured from the inferior rim of the mandibular canal to the lower border of the mandible
(a): : One-way ANOVA with adjustment for multiple comparisons of Bonferroni

Table 5 shows the group data of the four distances measured in the lower second molar on the left side. There was no significant difference between the Newtom3G, i-CAT and manual measurement in measuring distances AC (F=0.37, P=0.58), BC (F=0.52 P=0.60), LC (F=0.12, P=0.84) and IC (F=1.30, P=0.30). Distances AC and IC in the NewTom3G were slightly larger than those of the i-CAT and manual measurement while BC in the NewTom3G were slightly smaller than those of in the i-CAT and manual measurement. LC distance of the i-CAT was smallest in the three groups. However, these differences were not statistically significant.

1.3. At the region of the lower third molar

Table 6. Statistics of variables measured at the region of the right mandibular third molar.

Right Side	Mean±SD			P-value[(a)]
	NewTom 3G	i-CAT	DryM	
AC	12.62±1.04	12.66±0.52	11.45±0.64	0.19
BC	5.72±1.29	5.74±1.10	6.15±1.38	0.55
LC	3.61±1.01	3.82±1.26	3.98±1.26	0.15
IC	11.03±1.53	10.51±1.91	10.92±1.73	0.052

DryM : Dry Mandible
SD : Standard Deviation
AC : distance measured from the alveolar crest of the mandible to the superior border of the mandibular canal
BC : distance measured from the buccal rim of the mandibular canal to the buccal margin of the mandible
LC : distance measured from the lingual rim of the mandibular canal to the lingual margin of the mandible
IC : distance measured from the inferior rim of the mandibular canal to the lower border of the mandible
(a): : One-way ANOVA with adjustment for multiple comparisons of Bonferroni

Table 6 presents the group data of the four distances measured at the region of the lower third molar on the right side. The findings with one-way ANOVA analysis showed that manual measurement was not significantly different from the Newtom3G, i-CAT and in measuring distances consisting of AC (F=1.83, P=0.19), BC (F=0.61, P=0.55), LC (F=2.13, P=0.15) and IC (F=3.51, P=0.052). AC distances of the Newtom3G and i-CAT were higher than that of manual measurement. However, BC distance of the manual measurement was larger than that of the Newtom3G and i-CAT. In addition, LC of the

Newtom3G and IC of the i-CAT were smallest in the three groups compared. However, these differences were not statistically significant.

Table 7. Statistics of variables measured at the region of the left mandibular third molars.

Left Side	Mean±SD			P-value[(a)]
	NewTom 3G	i-CAT	DryM	
AC	12.16±2.49	12.34±1.72	11.54±2.77	0.21
BC	6.37±1.21	6.54±0.76	6.74±1.00	0.64
LC	3.68±1.45	3.64±1.45	3.76±1.54	0.94
IC	10.20±1.53	9.56±1.91	9.76±1.73	0.18

DryM : Dry Mandible
SD : Standard Deviation
AC : distance measured from the alveolar crest of the mandible to the superior border of the mandibular canal
BC : distance measured from the buccal rim of the mandibular canal to the buccal margin of the mandible
LC : distance measured from the lingual rim of the mandibular canal to the lingual margin of the mandible
IC : distance measured from the inferior rim of the mandibular canal to the lower border of the mandible
(a): : One-way ANOVA with adjustment for multiple comparisons of Bonferroni

Table 7 shows data of the four distances measured at region of the lower third molar on the left side. There was no significant difference between the Newtom3G, i-CAT, and manual measurement in the measured distances AC (F=1.81, P=0.21), BC (F=0.46, P=0.64), LC (F=0.06, P=0.94), and IC (F=1.87, P= 0.18). AC distance of the i-CAT was slightly larger than that of both the Newtom3G and manual measurement. BC distance of the i-CAT and manual measurement were slightly larger than those of the NewTom3G. LC for three groups was similar (F=0.06, P=0.94). However, these differences were not statistically significant.

2. Mean difference of distances measured at the region of the mandibular molars

2.1. At the region of the lower first molars

Horizontally, the mean difference for variables BC and LC measured at the region of the mandibular first molars for the NewTom3G, i-CAT and manual measurement ranged from 0.01 to 0.56 mm (table 8).

Vertically, the mean difference for variables AC and IC measured at the region of the mandibular first molars for the NewTom3G, i-CAT and manual measurement ranged from 0.05 to 0.57 mm (table 9).

2.2. At the region of the lower second molars

Horizontally, the mean difference for variables BC and LC measured at the region of the mandibular second molars using the NewTom3G, i-CAT and manual measurement ranged from 0.006 to 0.47 mm (table 10).

Vertically, the mean difference for variables AC and IC measured at the region of the mandibular second molars using the NewTom3G, i-CAT and manual measurement ranged from 0.01 to 0.54 mm (table 11).

2.3. At the region of the lower third molars

Horizontally, the mean difference for variables BC and LC measured at the region of the mandibular third molars using the NewTom3G, i-CAT and manual measurement ranged from 0.08 to 0.43 mm (table 12).

Vertically, the mean difference for variables AC and IC measured at the region of the mandibular third molars using the NewTom3G, i-CAT and manual measurement ranged from 0.04 to 0.64 mm, with the exception for the difference AC distances of 1.20 mm at site M_3 on the right side between CBVT system and Manual Measurement (table 13).

The findings in tables 8-13 showed that mean differences for distances measured between the NewTom3G, i-CAT and manual measurement ranged from 0.01 to 0.60 mm. In particular, in one case, the minimum difference was 0.006 mm between the i-CAT and manual measurement measured at the lower second molar on the right side. The maximum difference was up to 1.20 mm for AC distances measured at site M_3 on the right side between CBVT system and manual measurement.

Figures 29- 31 show the result of 240 distances measured for AC, BC, LC and IC on both the right and left sides in all three groups.

The mean difference between the manual measurement and that of the i-CAT was 0.11mm (t =1.72; P = 0.09; 95% Confidence Interval (CI): - 0.24 to 0.02). The mean difference between the manual measurement and the Newtom3G was 0.03mm (t = 0.34; 95% CI: - 0.20 to 0.14). The measured parameters of the Newtom3G were 0.08 mm larger than those of the i-CAT (t = 1.04; P = 0.30; 95% CI: - 0.07 to 0.24). However, these differences were not statistically significant.

From the findings, it can be assumed that the distances measured on both NewTom3G and i-CAT underestimate those obtained by manual measurement. Likewise, the distances measured by the i-CAT were less when compared with the NewTom3G.

Table 8. Paired mean difference of variables BC and LC measured at the region of the lower first molars from the NewTom3G, i-CAT and manual measurement.

Pairs of variables measured		Mean Difference	SEM	95% CI		P-value [(a)]
$BCM_1L(1)$	$BCM_1L(2)$	-0.10	0.26	-0.87	0.65	1.00
$BCM_1L(2)$	$BCM_1L(3)$	-0.24	0.20	-0.84	0.35	0.77
$BCM_1L(3)$	$BCM_1L(1)$	0.34	0.32	-0.61	1.30	0.95
$BCM_1R(1)$	$BCM_1R(2)$	-0.07	0.07	-0.27	1.26	0.96
$BCM_1R(2)$	$BCM_1R(3)$	-0.49	0.18	-1.01	0.02	0.06
$BCM_1R(3)$	$BCM_1R(1)$	0.56	0.17	0.06	1.06	$0.03^{(*)}$
$LCM_1L(1)$	$LCM_1L(2)$	0.01	0.16	-0.46	0.48	1.00
$LCM_1L(2)$	$LCM_1L(3)$	-0.12	0.36	-1.45	1.21	1.00
$LCM_1L(3)$	$LCM_1L(1)$	0.11	0.16	-1.02	1.24	1.00
$LCM_1R(1)$	$LCM_1R(2)$	-0.33	0.31	-1.48	0.82	1.00
$LCM_1R(2)$	$LCM_1R(3)$	-0.12	0.36	-1.45	1.21	1.00
$LCM_1R(3)$	$LCM_1R(1)$	0.45	0.51	-1.43	2.33	1.00

(a) : ANOVA with adjustment for multiple comparisons of Bonferroni
R : Right side, L: Left side
M_1 : site of the first molar
(1) : NewTom3G
(2) : i-CAT
(3) : DryM: Dry Mandible
SEM : Standard Error of Mean

Table 9. Paired mean difference of variables AC and IC measured at the region of the lower first molars from the NewTom3G, i-CAT and manual measurement.

Pairs of variables measured		Mean Difference	SEM	95% CI		P-value [(a)]
$ACM_1L(1)$	$ACM_1L(2)$	-0.57	0.41	-1.36	2.16	0.84
$ACM_1L(2)$	$ACM_1L(3)$	-0.55	0.73	-2.68	1.59	1.00
$ACM_1L(3)$	$ACM_1L(1)$	-0.40	0.71	-2.49	1.69	1.00
$ACM_1R(1)$	$ACM_1R(2)$	-0.24	0.57	-1.92	1.44	1.00
$ACM_1R(2)$	$ACM_1R(3)$	0.51	0.31	-0.41	1.44	0.47
$ACM_1R(3)$	$ACM_1R(1)$	-0.27	0.47	-1.66	1.11	1.00
$ICM_1L(1)$	$ICM_1L(2)$	-0.07	0.31	-0.98	0.84	1.00
$ICM_1L(2)$	$ICM_1L(3)$	-0.48	0.25	-1.22	0.25	0.26
$ICM_1L(3)$	$ICM_1L(1)$	0.55	0.27	-0.25	1.36	0.22
$ICM_1R(1)$	$ICM_1R(2)$	0.47	0.26	-0.30	1.24	0.33
$ICRM_1(2)$	$ICM_1R(3)$	-0.41	0.23	-1.09	0.26	0.23
$ICM_1R(3)$	$ICM_1R(1)$	-0.05	0.43	-1.32	1.21	1.00

(a) : ANOVA with adjustment for multiple comparisons of Bonferroni
R : Right side, L: Left side
M_1 : site of the first molar
(1) : NewTom3G
(2) : i-CAT
(3) : DryM: Dry Mandible
SEM : Standard Error of Mean

Table 10. Paired mean difference of variables measured at the region of the lower second molars from the NewTom3G, i-CAT and manual measurement.

Pairs of variables measured		Mean Difference	SEM	95% CI		P-value[(a)]
$BCM_2L(1)$	$BCM_2L(2)$	-0.03	0.19	-0.60	0.54	1.00
$BCM_2L(2)$	$BCM_2L(3)$	-0.19	0.23	-0.54	0.60	1.00
$BCM_2L(3)$	$BCM_2L(1)$	0.22	0.26	-0.53	0.97	1.00
$BCM_2R(1)$	$BCM_2R(2)$	0.14	0.34	-0.86	1.14	1.00
$BCM_2R(2)$	$BCM_2R(3)$	-0.47	0.14	-0.48	0.04	0.02[(*)]
$BCM_2R(3)$	$BCM_2R(1)$	0.33	0.27	-0.48	1.14	0.79
$LCM_2L(1)$	$LCM_2L(2)$	-0.11	0.47	-1.49	1.27	1.00
$LCM_2L(2)$	$LCM_2L(3)$	-0.13	0.20	-0.71	0.45	1.00
$LCM_2L(3)$	$LCM_2L(1)$	0.24	0.42	-0.99	1.47	1.00
$LCM_2R(1)$	$LCM_2R(2)$	-0.18	0.19	-0.60	0.23	0.71
$LCM_2R(2)$	$LCM_2R(3)$	-0.006	0.11	-0.34	0.33	1.00
$LCM_2R(3)$	$LCM_2R(1)$	0.19	0.25	-0.30	0.68	0.88

(a) : ANOVA with adjustment for multiple comparisons of Bonferroni
R : Right side, L: Left side
M_2 : site of the second molar
(1) : NewTom3G
(2) : i-CAT
(3) : DryM: Dry Mandible
SEM : Standard Error of Mean

Table11. Paired mean difference of variables AC and IC measured at the region of the lower second molars from the NewTom3G, i-CAT and manual measurement.

Pairs of variables measured		Mean Difference	SEM	95% CI		P-value [(a)]
$ACM_2L(1)$	$ACM_2L(2)$	0.36	0.67	-0.13	0.85	0.17
$ACM_2L(2)$	$ACM_2L(3)$	0.01	0.56	-1.62	1.65	1.00
$ACM_2L(3)$	$ACM_2L(1)$	-0.37	0.62	-2.2	1.46	1.00
$ACM_2R(1)$	$ACM_2R(2)$	0.15	1.06	-2.97	3.27	1.00
$ACM_2R(2)$	$ACM_2R(3)$	-0.11	0.32	-1.03	0.82	1.00
$ACM_2R(3)$	$ACM_2R(1)$	-0.04	1.01	-3.00	2.92	1.00
$ICM_2L(1)$	$ICM_2L(2)$	0.54	0.45	-0.78	1.85	0.77
$ICIM_2L(2)$	$ICM_2L(3)$	-0.47	0.32	-1.42	0.48	0.54
$ICM_2L(3)$	$ICM_2L(1)$	-0.07	0.31	-0.98	0.84	1.00
$ICM_2R(1)$	$ICM_2R(2)$	0.40	0.47	-0.99	1.79	1.00
$ICM_2R(2)$	$ICM_2R(3)$	-0.25	0.36	-1.29	0.79	1.00
$ICM_2R(3)$	$ICM_2R(1)$	-0.15	0.24	-0.85	0.55	1.00

(a) : ANOVA with adjustment for multiple comparisons of Bonferroni
R : Right side, L: Left side
M_2 : site of the second molar
(1) : NewTom3G
(2) : i-CAT
(3) : DryM: Dry Mandible
SEM : Standard Error of Mean

Table 12. Paired mean difference of variables BC and LC measured at the region of the lower third molar from the NewTom3G, i-CAT and manual measurement.

Pairs of variables measured		Mean Difference	SEM	95% CI		P-value[(a)]
$BCM_3L(1)$	$BCM_3L(2)$	-0.17	0.45	-1.48	1.14	1.00
$BCM_3L(2)$	$BCM_3L(3)$	-0.20	0.18	-0.75	0.38	0.89
$BCM_3L(3)$	$BCM_3L(1)$	0.37	0.47	-1.01	1.76	1.00
$BCM_3R(1)$	$BCM_3R(2)$	-0.20	0.45	-1.34	1.30	1.00
$BCM_3R(2)$	$BCM_3R(3)$	-0.41	0.43	-1.66	0.84	1.00
$BCM_3(3)$	$BCM_3R(1)$	0.43	0.45	-0.89	1.75	1.00
$LCM_3L(1)$	$LCM_3L(2)$	0.04	0.40	-1.14	1.22	1.00
$LCM_3L(2)$	$LCM_3L(3)$	-0.12	0.13	-0.50	0.26	1.00
$LCM_3L(3)$	$LCM_3L(1)$	0.08	0.46	-1.26	1.43	1.00
$LCM_3R(1)$	$LCM_3R(2)$	-0.21	0.19	-0.78	0.36	0.93
$LCM_3R(2)$	$LCM_3R(3)$	-0.16	0.15	-0.59	0.27	0.94
$LCM_3R(3)$	$LCM_3R(1)$	0.37	0.19	-0.19	0.92	0.25

(a) : ANOVA with adjustment for multiple comparisons of Bonferroni
R : Right side, L: Left side
M_3 : site of the third molar
(1) : NewTom3G
(2) : i-CAT
(3) : DryM: Dry Mandible
SEM : Standard Error of Mean

.

Table13. Paired mean difference of variables AC and IC measured at the region of the third lower molars from the NewTom3G, i-CAT and manual measurement.

Pairs of variables measured		Mean Difference	SEM	95% CI		P-value [(a)]
$ACM_3L(1)$	$ACM_3L(2)$	-0.18	0.39	-1.34	0.98	1.00
$ACM_3L(2)$	$ACM_3L(3)$	0.58	0.57	-0.92	2.48	0.63
$ACM_3L(3)$	$ACM_3L(1)$	-0.60	0.25	-1.33	0.13	0.13
$ACM_3R(1)$	$ACM_3R(2)$	-0.04	0.75	-2.26	2.17	1.00
$ACM_3R(2)$	$ACM_3R(3)$	1.20	0.64	-0.68	3.09	0.28
$ACM_3R(3)$	$ACM_3R(1)$	-1.17	0.75	-3.36	1.03	0.46
$ICM_3L(1)$	$ICM_3L(2)$	0.64	0.37	-0.43	1.71	0.34
$ICM_3L(2)$	$ICM_3L(3)$	-0.20	0.19	0.76	0.36	0.98
$ICM_3L(3)$	$ICM_3L(1)$	-0.44	0.34	-1.44	0.55	0.68
$ICM_3R(1)$	$ICM_3R(2)$	0.52	0.21	-0.11	1.15	0.12
$ICM_3R(2)$	$ICM_3R(3)$	-0.41	0.18	-0.95	0.14	0.17
$ICM_3R(3)$	$ICM_3R(1)$	-0.11	0.22	-0.75	0.52	1.00

(a) : ANOVA with adjustment for multiple comparisons of Bonferroni
R : Right side, L: Left side
M_3 : site of the third molar
(1) : NewTom3G
(2) : i-CAT
(3) : DryM: Dry Mandible
SEM : Standard Error of Mean

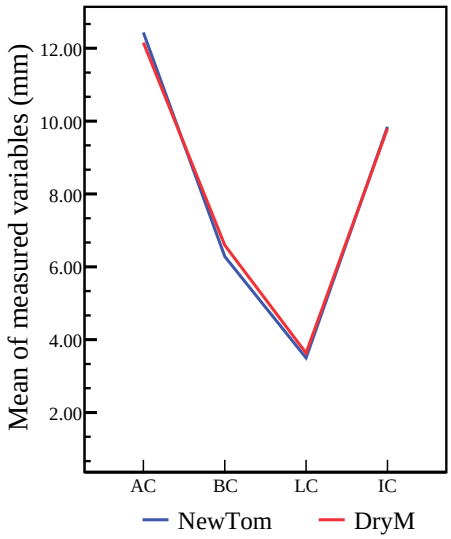

Figure 29. The Newtom3G shows a strong linear correlation with the manual measurement although variables measured on the Newtom3G were less than those of the manual measurement.

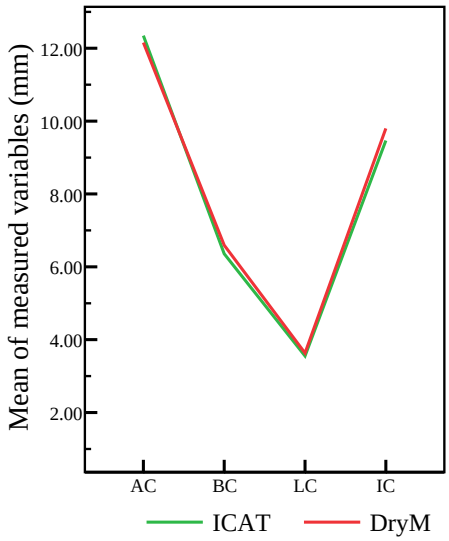

Figure 30. The i-CAT shows a strong linear correlation with the manual measurement although variables measured on the i-CAT were less than those of the manual measurement.

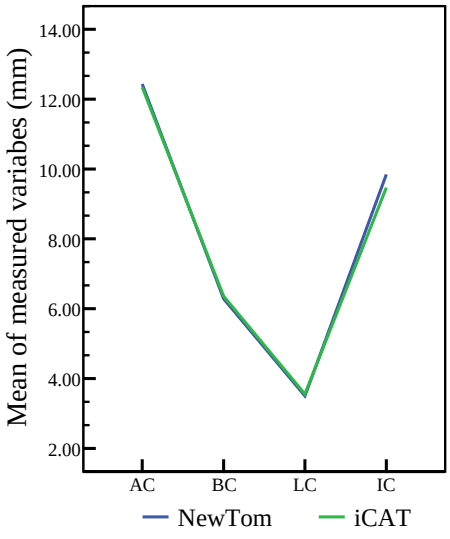

Figure 31. The Newtom3G shows a strong linear correlation with the i-CAT although variables measured on the i-CAT were less than those of the Newtom3G.

3. The course of the mandibular canal in the mandible on right and left sides

In order to compare the course of the mandibular canal on the left and right sides, three sites M_1, M_2 and M_3 at the regions of the first, second and third molars respectively were assessed by using t-test to analyze the distances measured of AC, BC, LC and IC.

3.1. *Comparison of measured variables between the right and left sides in the region of the first molar*

Figures 32, 33 and 34 shows the data of distances measured at the regions of the right and left mandibular first molar where the AC distance on the right side was slightly smaller than that of the left side. In contrast, BC and LC at the right first molar were slightly larger than those of the left first molar area. However, IC on both sides was variable.

AC distance

AC distance measured by the Newtom3G (Fig 32) with the analysis result of the t-test showed that there was significant difference in distances measured between left and right sides ($t = 2.29$, $P = 0.048^*$; 12.38 versus 13.97mm; 95% CI: - 3.16 to -0.02). In contrast, AC distance measured by the i-CAT and manual measurement was found to have no significant difference between distances measured from the right and left sides at the region of the first molar ($t = 0.63$, $P = 0.54$; 12.62 versus 13.02mm; 95% CI: from -1.83 to 1.03 and $t = 1.47$, $P = 0.18$; 12.10 versus 13.57mm; 95% CI: from -3.72 to 0.79 for the i-CAT and manual measurement, respectively).

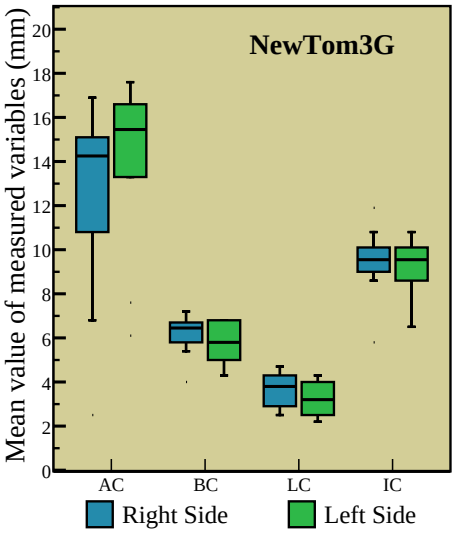

Figure 32. Comparison of the distances measured AC, BC, LC and IC between the right and left sides at the region of the first molar using the NewTom3G.

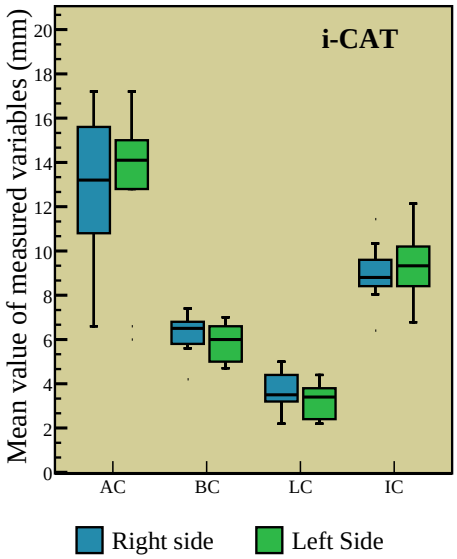

Figure 33. Comparison of the distances measured AC, BC, LC and IC between the right and left sides at the region of the first molar using the i-CAT.

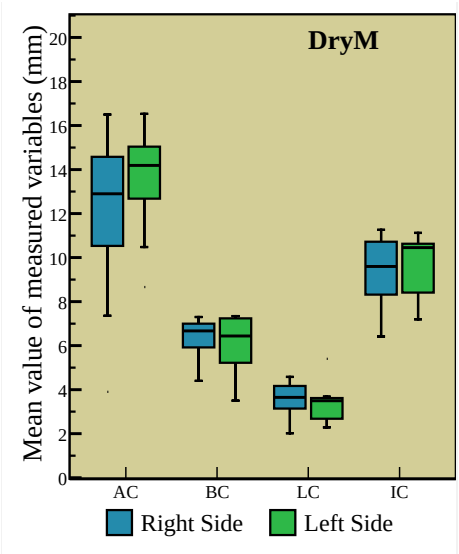

Figure 34. Comparison of the distances measured AC, BC, LC and IC between the right and left sides at the region of the first molar from the manual measurement. DryM: Dry Mandible.

BC distance

BC distance measured on the NewTom3G with analysis of t-test showed that on mean difference, BC at the right side of the first molar region was 0.43mm larger than that of at the left side. However, this difference was not statistically significant (t = 1.37, P = 0.20; 6.20 versus 5.75mm; 95% CI: - 0.28 to 1.14). Similarly, BC distance measured at the first molar region on the right side on both the i-CAT and manual measurement were 0.40mm and 0.29mm respectively larger than those of on the left side. These differences were also considered not significant (For the i-CAT: t = 1.30; P = 0.23; 6.25 versus 5.85mm; 95% CI: from -0.29 to 1.10 and t = 0.76, P = 0.47; 6.38 versus 6.09mm; 95% CI: from -0.57 to 1.14 for the manual measurement).

LC distance

LC distance measured on the NewTom3G with analysis of t-test showed that on mean difference, LC distance on the right side of the first molar region was 0.48mm larger than that of the left side. However, this difference was considered not significant (t = 1.69; P = 0.12; 3.71 versus 3.23mm; 95% CI: from -0.16 to 1.12). Similarly, LC distance measured on the i-CAT and the manual measurement at the region of the first molar on the right side were 0.40mm and 0.21mm respectively larger than those of the left side. These differences were not significant (For the i-CAT: t = 1.96; P = 0.08; 3.62 versus 3.22mm; 95% CI: from -0.06 to 0.86 and t = 0.47; P = 0.65; 3.55 versus 3.34mm; 95% CI: from -0.81 to 1.24 for the manual measurement).

IC distance

IC distance measured on the NewTom3G with analysis of t-test showed that on mean difference IC distance at the region of the first molar on the right side was 0.12mm larger than that of the left side. However, this difference was not significant (t = 0.51; P = 0.62; 9.44 versus 9.17mm; 95% CI: from -0.92 to 1.46). In contrast, IC distance measured from the i-CAT at the region of the first molar on the right side was 0.27mm smaller than that of the left side (t = -0.46; P = 0.66; 8.97 versus 9.24mm; 95% CI: from -0.33 to 1.45). In addition, IC distance measured by manual measurement at the region of the first molar on the right side was 0.34 smaller than that of the left side (t = -0.74; P = 0.45; 9.38vs 9.9.72mm; 95% CI: from - 1.37to 0.67).

3.2.*Comparison of measured variables between the right and left sides in the region of the second molar*

Figures 35, 36 and 37 showed the data of distances measured at the second molar area on the right and left sides where the AC distance at the right second molar area was slightly smaller than that of the left side. In contrast, BC, LC and IC distances measured at the region of the second molar on the right side were slightly larger than those of the left side.

AC distance

AC distance measured at the region of the second molar on the right side by the Newtom3G was 0.65mm smaller than that of the left side, but the analysis result of t-test showed this difference was not statistically significant (t = -0.87; P = 0.41; 11.83mm versus 12.48mm; 95% CI: from -2.35 to 1.05). Similarly, the AC distance measured at the region of the second molar on the right side on the i-CAT was 0.44mm smaller than

that of the left side. However, this difference was not statistically significant (t = -0.67; P = 0.53; 11.68mm versus 11.12mm; 95% CI: from -1.95 to 1.07).

For the manual measurement, the findings show that there was not significant difference in AC distances measured between the right and left sides though this distance on the right side was smaller by 0.32mm than that of the left side (t = -0.36; P = 0.73; 11.78mm versus 12.10mm; 95% CI: from -2.33 to 1.67).

BC distance

On the mean difference, BC distance measured at the area of the right second molar on the NewTom3G was 0.34mm larger than that on the left side. However, this difference was not significant (t = 1.94; P = 0.08; 7.07mm versus 6.70mm; 95% CI: from -0.14 to 0.88). Similarly, BC distance measured at the region of the right second molar both the i-CAT and manual measurement was 0.37mm and 0.40mm respectively larger than that on the left side. However, these differences were also not considered significant (for the i-CAT: t = 1.64; P = 0.13; 7.07mm versus 6.70mm; 95% CI: from -0.14 to 8.88 and t = 1.58, P = 0.15; 7.29mm versus 6.89mm; 95% CI: from -0.17 to 0.98, for the manual measurement).

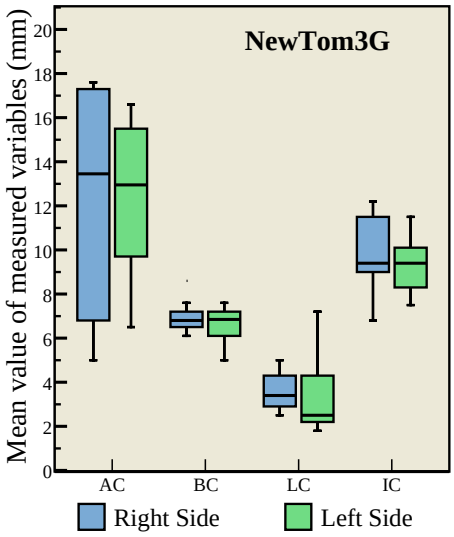

Figure 35. Comparison of the distances measured AC, BC, LC and IC at the region of the second molar between the right and left side on the Newtom3G.

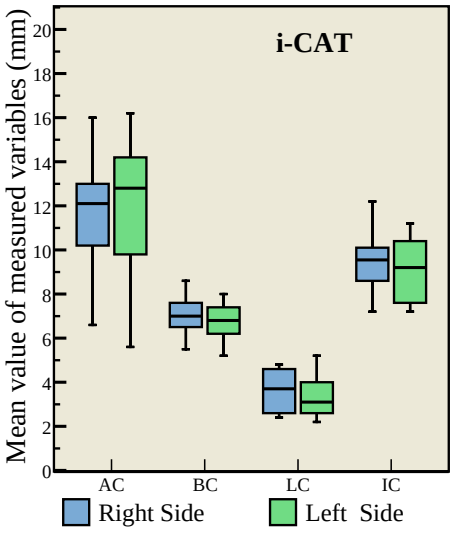

Figure 36. Comparison of the distances measured AC, BC, LC and IC between the right and left sides at the region of the second molar on the i-CAT.

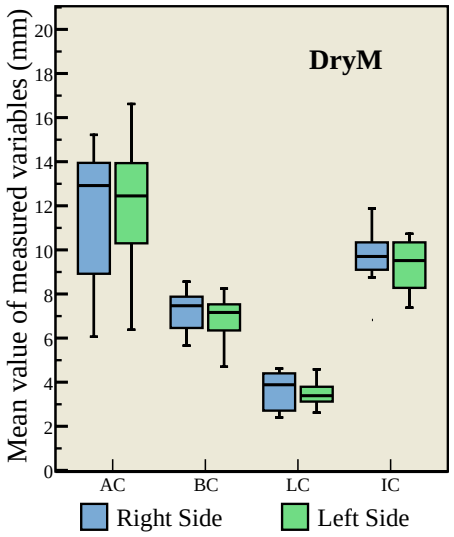

Figure 37. Comparison of the distance measured AC, BC, LC and IC on the right and left sides at the region of the second molar from the manual measurements

LC distance

For the NewTom3G, the findings of the analysis t-test showed that on the mean difference LC distance measured at the region of the right second molar was 0.21mm smaller than that on the left side although this difference was not significant (t = -0.42; P = 0.69; 3.28mm versus 3.49mm; 95% CI: from -1.35 to 0.93). In contrast, LC distances measured by the i-CAT and manual measurement on the right side were 0.30mm and 0.17mm respectively larger than those on the left side. However, these differences were not significant (for i-CAT: t = 0.94; P = 0.37; 3.66mm versus 3.36mm; 95% CI: from -0.42 to 1.02 and t = 0.64 P = 0.54; 3.67mm versus 3.49mm; 95% CI: from -0.44 to 0.79 for the manual measurement).

IC distance

On the mean difference, IC distance measured at the region of the right second molar from the NewTom3G was 0.49mm larger than that of the left side. However, with analysis of t-test, this difference was not significant (t = 0.84; P = 0.42; 9.86mm versus 9.37 mm; 95% CI: from -0.83 to 1.81. Similarly, this distance measured at the region of the right second molar on the i-CAT was 0.40 mm larger than that on the left side (t = 1.05; P =0.32; 9.46mm versus 9.06mm; 95% CI: from -0.46 to 1.26). LC distance measured at the region of the second molar on the manual measurement on the right side was 0.31mm larger than that on the left side (t =0.88, P= 0.40; 9.71mm versus 9.30mm; 95% CI: from -0.64 to 1.45).

3.3. *Comparison of measured variables between the right and left sides in the region of the third molar*

Figures 38, 39 and 40 showed the data of distances at the region of the mandibular third molar on the right and left sides. These figures showed that AC and BC distances measured at the region of the right third molar were slightly smaller than those on the left side. In contrast, LC and IC distances measured at the region of the third right molar were slightly larger than those on the left side.

AC distance

On the mean difference, AC distance measured at the region of the right third molar on the Newtom3G was 0.38mm smaller than that on the left side although this difference was considered not statistically significant (t = - 0.04; P = 0.69; 11.78mm versus 12.16mm; 95% CI: from -2.46 to1.70). Similarly, AC distance measured at the region of the right third molar on the i-CAT was 0.05 mm smaller than that on the left side and this difference was not statistically significant in distances measured between right and left sides (t = - 0.07; P = 0.94; 12.29mm versus 12.34mm; 95% CI: from -1.55 to 1.46. In contrast, this distance measured from the manual measurement on the right was 0.25 mm smaller than that on the left side although there was no significant difference between right and left sides (t = 0.33; P = 0.75; 11.81mm versus 11.56mm; 95% CI: from - 1.48 to 1.99).

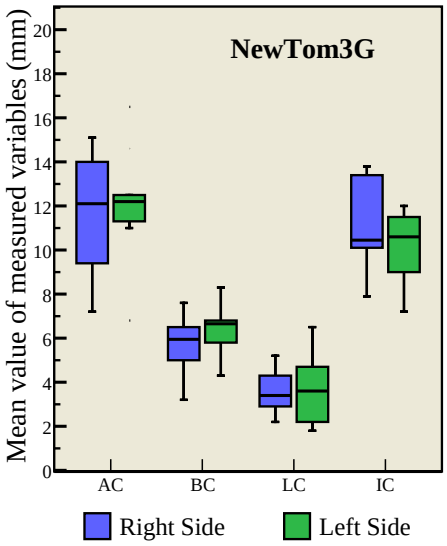

Figure 38. Comparison of the distances measured AC, BC, LC and IC at the region of the third molar on the right and left sides using the NewTom3G.

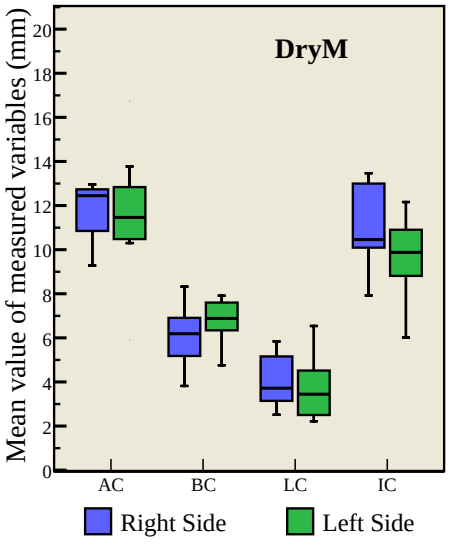

Figure 39. Comparison of the distances measured AC, BC, LC and IC at the region of the third molar on the right and left sides on the dry mandible.

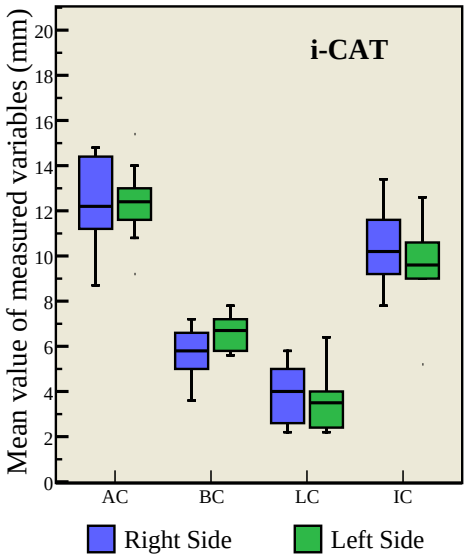

Figure 40. Comparison of the distances measured AC, BC, LC and IC at the region of the third molar on the right and left sides using the i-CAT.

BC distance

On the mean difference, BC distance measured at the region of the right third molar on the NewTom3G was 0.65mm smaller than that on the left side. However, this difference was not significant (t = -1.28; P = 0.23; 5.72mm vs 6.37mm; 95% CI: from -1.80 to 0.50). Similarly, BC distances on the i-CAT and manual measurement at the area of the right third molar were 0.80mm and 0.59mm respectively smaller than that on the left side. However, these differences were not considered significant (for the i-CAT: t = -2.12; P = 0.06; 5.74m vs 6.54mm; 95% CI: from -1.65 to 0.05 and t = -1.43; P = 0.19; 6.15mm vs 6.74mm; 95% CI: from -1.52 to 0.34 for the manual measurement).

LC distance

LC distance measured at the region of the right third molar on the NewTom3G with analysis of t-test on the mean difference was 0.07 mm smaller than that on the left side. However, this difference is not significant (t = - 0.21; P = 0.84; 3.61mm versus 3.68mm; 95% CI: from - 0.81 to 0.67). In contrast, LC distances measured at the region of the right third molar on both the i-CAT and manual measurement were 0.18 mm and 0.21 mm respectively larger than those on the left side in the third molar region. However, these differences were not significant (for the i-CAT: t = 0.62; P = 0.55; 3.82 mm versus 3.64 mm; 95% CI: from - 0.47 to 0.83 and t = 0.65; P = 0.53; 3.98 versus 3.76 mm; 95% CI: from - 0.53 to 0.96 for the manual measurement).

IC distance

For the NewTom3G, with analysis of t-test, IC distance measured at the region of the right third molar was 0.83mm larger than that on the left side. However, this difference

was not significant (t = 1.54; P = 0.16; 11.03 mm versus 10.20 mm; 95% CI: from - 0.38 to 2.04). Similarly, on the mean difference, IC distance measured at the region of the right third molar on the i-CAT was 0.95 mm larger than that on the left side (t = 1.63; P = 0.14; 10.51 mm versus 9.56 mm; 95% CI: from-0.36 to 2.26). On the other hand, IC from the manual measurement was 1.15 mm larger that on the left side and this difference was statistically significant on both sides (t = 2.24; P = 0.04*; 10.92 mm versus 9.76 mm; 95%CI: from 0.08 to 2.23).

4. Difference between the Orthophos and CBVT systems

4.1. At the region of the lower first molars

On the right side of the mandible, IC distances measured at the region of the first molar with the analysis of one-Way ANOVA showed that there was statistically significant difference among the four variables measured on the Newtom3G, i-CAT, manual measurement and Orthophos (F=32.33, P<0.001). Similarly, the findings showed that there was statistically significant difference among IC distances measured at the region of the second molar on the left side using the Newtom3G, i-CAT, manual measurement and Orthophos (F=15.32, P<0.001).

Table 14 shows the mean differences of pair comparisons of IC distances measured at the region of the second mandibular molar on both sides of which differences of IC distances measured between Orthophos and the manual measurement; NewTom3G as well as the i-

CAT on the right side were 1.89, 1.77 and 2.29 mm, respectively. Similarly, these differences of IC distances measured on the left side were 0.93, 1.19 and 2.15 mm, respectively.

Table 14. IC distances were measured in the bilateral first molar regions: between Orthophos OPG and Manual Measurement (DryM); between Othorphos and NewTom 3G; between Orthophos and i-CAT.

IC (mm)	Mean Differences	95%CI	P (a)
Ortho-NT3G(R)	1.77*	0.64 to 2.91	0.003*
Ortho-i-CAT(R)	2.29*	1.86 to 2.72	0.000*
Ortho-DryM (R)	1.89*	1.27 to 2.51	0.000*
Ortho- NT3G(L)	1.19*	0.60 to 1.78	0.000*
Ortho-i-CAT(L)	2.15*	1.00 to 3.30	0.001*
Ortho-DryM(L)	0.93*	0.17 to 1.70	0.016*

DryM : Dry Mandible
NT3G : NewTom 3G
R : Right side; L: Left side
IC : from the inferior rim of the canal to the lower border of the mandible
(a) : adjustment for multiple comparisons of Bonferroni.
(*) : the mean difference is significant at the 0 .05 level

4.2. At the region of the lower second molars

On the left side of the mandible, IC distances measured at the region of the second molar with the analysis of one-Way ANOVA showed that there was a statistically significant difference among the four variables measured from the Newtom3G, i-CAT, manual measurement and Orthophos ($F=20.58$, $P<0.001$). Similarly, the findings showed that there were statistically significant differences among the IC distances measured at the

region of the second molar on the right side on the Newtom3G, i-CAT, manual measurement and Orthophos (F=22.68, P<0.001).

Table 15. IC distances were measured in the second molar region on both sides using Orthophos OPG and manual measurement; between Othorphos and NewTom 3G; between Orthophos and i-CAT.

IC (mm)	Mean Differences	95%CI	P(a)
Ortho-NT3G(R)	1.75*	0.55 to 2.95	0.005*
Ortho-i-CAT(R)	2.21*	1.55 to 2.87	0.000*
Ortho-DryM (R)	1.50*	0.81 to 2.18	0.000*
Ortho- NT3G(L)	1.61*	0.52 to 2.69	0.005*
Ortho-i-CAT(L)	2.12*	1.35 to 2.87	0.000*
Ortho-DryM(L)	1.23*	0.23 to 2.23	0.015*

DryM : Dry Mandible
NT3G : NewTom 3G
R : Right side; L: Left side
IC : from the inferior rim of the canal to the lower border of the mandible
(*) : adjustment for multiple comparisons of Bonferroni
(a) : the mean difference is significant at the 0 .05 level

Table 15 shows the mean differences of pair comparisons of the IC distances measured at the region of the second molars on the both sides. The IC distances measured between the Orthophos and the NewTom3G, the i-CAT and the manual measurement, on the right side were 1.75, 2.21 and 1.50 mm respectively. Similarly, these differences of the IC distances measured on the left side were 1.61, 2.12 and 1.23 mm, respectively.

4.3. At the region of the lower third molars

Table 16: IC distances were measured bilaterally in the third molar regions between Orthophos OPG and manual measurement; between Othorphos and NewTom 3G; between Orthophos and i-CAT.

IC (mm)	Mean Differences	95%CI	P (a)
Ortho-NT3G(R)	1.35*	0.28 to 2.41	0.013*
Ortho-i-CAT(R)	2.05*	1.21 to 2.89	0.000*
Ortho-DryM (R)	1.33*	0.24 to 2.42	0.016*
Ortho- NT3G(L)	1.19*	0.51 to 1.87	0.001*
Ortho-i-CAT(L)	1.77*	1.13 to 2.41	0.001*
Ortho-DryM(L)	1.62*	1.02 to 2.22	0.000*

DryM : Dry Mandible
NT3G : NewTom 3G
R : Right side; L: Left side
IC : from the inferior rim of the canal to the lower border of the mandible
(a) : adjustment for multiple comparisons of Bonferroni
(*) : the mean difference is significant at the 0 .05 level

On the right side of the mandible, the IC distances measured at the region of the third molars with the analysis of one-Way ANOVA showed that there was a statistically significant difference among the four variables measured from the Newtom3G, i-CAT, manual measurement and Orthophos ($F=21.20$, $P<0.001$). Similarly, the findings showed that there were statistically significant differences among the IC distances measured at the region of the second molar on the left side from the Newtom3G, i-CAT, manual measurement and the Orthophos ($F=26.32$, $P<0.001$).

Table 16 shows the mean differences of pair comparisons of the IC distances measured at the region of the third molar on the both sides. The IC distances measured between the Orthophos and the NewTom3G, the i-CAT and the manual measurement, on the right side were 1.35, 2.05 and 1.33mm respectively. Similarly, these differences of the IC distances measured on the left side were 1.62, 1.19 and 1.77 mm, respectively.

In summary, the findings showed that there was significant difference between the Orthophos, the NewTom3G and i-CAT. The significant difference between the Orthophos and the NewTom3G was 1.19 mm of the minimum difference and 1.77 mm of the maximum difference. Additionally, the significant difference between the Orthophos and the i-CAT was 1.77 mm being the minimum difference and 2.29 mm being the maximum difference.

5. LC at edentulous and dentate positions

There were 69 dentate positions and 161 edentulous positions collected and measured from the manual measurement at four sites $M_{0,}$ $M_{1,}$ M_2 and M_3 on the both sides of the mandible. The findings showed that there was significantly different of the LC distance measured between edentulous and dentate regions (Fig 41). (t = 7.49, Mean Difference: 1.02, 2.83mm (SD: 0.72) versus 3.85mm (SD: 1.01); P = 0.005; 95% CI: from 0.75 to 1.29).

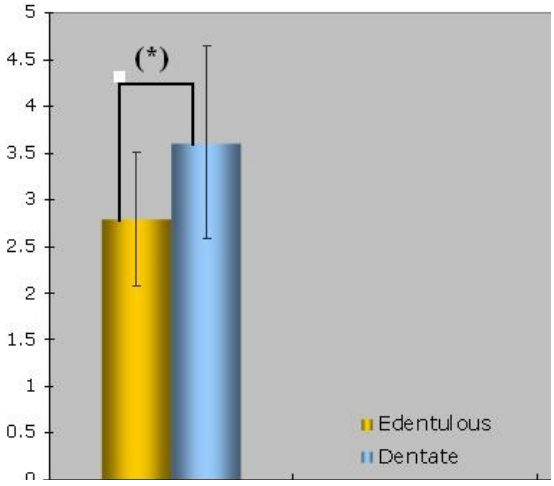

Figure 41. Mean (±SD) of LC distance at edentulous and dentate positions of the mandibles
(*) : Significant difference with t-test

6. Bone width of the mandible at the regions of the first, second and third molars bilaterally

Table 17. Bone width (BW) distances measured at the mandible on the right and left side

BW	Right side	Left Side	Mean difference	95% CI	P-value
First molar	12.15±1.09	11.55±1.49	0.60	0.15-1.06	0.01(*)
Second molar	12.88±1.41	12.47±1.48	0.41	-0.01-0.83	0.052
Third molar	12.50±2.05	12.47±1.99	0.02	-1.30-1.34	0.97

BW: distance measured from the lingual margin of the mandible to the buccal margin of the mandible. **(*)** : Significant difference with t-test

Table 17 showed that on average BW distance measured at the region of the first molar on the right was 0.6 mm larger than that of on the left side, and this difference was statistically significant (P=0.01<0.05). In addition, BW distances measured at the second

and third molars on the right side were 0.41 and 0.02 mm respectively larger than those on the left side. However, these differences were not statistically significant.

Chapter 4

DISCUSSION

Summary

Briefly, the aims of this study were:

- to evaluate the level of accuracy of the CBVT system by comparing measurements on the NewTom3G and i-CAT machines with manual measurements
- to determine the course of the mandibular canal in the regions of the first, second and third molars
- to compare the course of the mandibular canal on the right (R) and left (L) sides
- to compare measured variables between the CBVT and conventional panoramic units
- to determine appropriate positions for the implant placement at the region of the mandibular molar in relation to the mandibular canal.

In the present study, characteristics of the Newtom3G and i-CAT machines were investigated towards answering the question ‘what, how, and why CBVT is different from conventional CT and the panoramic system’. This will be discussed in the following paragraphs.

The findings of this study showed that there was no a significant difference, in most cases, in the variables measured from the NewTom3G, i-CAT machines and manual measurement.

This clearly demonstrated that CBVT is an accurate diagnostic tool for locating the course of the mandibular canal. In the present study, the results suggested that the course of the mandibular canal on the right and left sides was slightly different, but not statistically significant ($P>0.05$). It appears that the course of the mandibular canal on the right and left sides of the mandible was variable.

On the other hand, there was significant statistical difference between the Orthophos OPG machine and CBVT system ($P=0.00<0.05$). The difference of measured variables between CBVT and OPG machines varied from 1.19 mm to 2.29 mm.

In terms of dental clinical application, the distances measured in other aspects of the correlation between the mandibular canal and the mandible which were summarized in table 12 were likely to be valuable references when making a pre-surgical assessment in the regions of the mandibular molars.

Data of LC distances measured at edentulous and dentate molar regions were analysed and found that there were significant difference between edentulous and dentate molar regions ($P<0.001$). A further evaluation of this at other distances such as BC, IC should be investigated to properly obtain consistent results.

1. What is the level of accuracy of the CBVT?

The findings showed that there was no significant difference in distances measured between the CBVT system and manual measurement. However, it was assumed that the results from the CBVT were slightly underestimated in terms of measurement when compared to manual measurements. In particular, distances measured from the i-CAT machine appear to be smallest among the three-group data. This finding

was similar to a previous report by Lascala in which distances measured on eight skulls were carried out to evaluate the accuracy of images from the NewTom 9000 and Hitachi MercuRay units, given that the real measurements were larger than those measured from CBVT images, but this difference was not statistically significant [93].

In a recent study, Stratemann et al stated that the CBVT system (NewTom® QR DVT 9000 and Hitachi MercuRay) was highly accurate, with less than 1% relative error compared to direct physical measurements [94]. Moreover, their study showed that the NewTom 9000 was significantly different from both the physical measurement and MercuRay when 120 distances were measured. They also stated that this difference was below the level of clinical significance for orthodontic evaluations. It was explained by the difference from the grayscales between 12 Bit Grey Scale of Hitachi MercuRay versus 8 Bit Grey Scale of NewTom 9000. In the present study, the findings showed that on average, there was not statistically significant difference when 240 distances were measured among the NewTom3G, i-CAT and manual measurement. It is important to note that in this study sample size could be a factor contributing to the apparent accuracy of measurements. In another study, Christian et al found that difference of distances measured between conventional CT and physical measurements was 0.51±1.91mm [2]. In the present study, the mean difference between the CBVT and manual measurement found were 0.03 and 0.11 mm for the NewTom3G and i-CAT, respectively, when 240 distances were measured. It appeared that the measurements were more accurate in CBVT than in conventional CT. This difference was probably attributed to the difference in the isotropic voxel structure in the CBVT and the anisotropic voxel structure in conventional CT [69].

Another crucial point to note is that the tip of an implant placed in the region of the mandibular molars must be a minimum distance of 1mm from the mandibular canal. This should be assessed prior to surgical procedure [95, 96]. In the present study, the mean differences in all cases when comparing CBVT with manual measurement were less than 1mm. This demonstrated that CBVT is an accurate diagnostic tool for an assessment of the relationship between an implant placed in the region of the lower molars and the mandibular canal.

CBVT units have used the image intensifier tube/ charged-couple devise system or the flat-panel image system. The difference between these two systems could lead to differentiation of the image noise [98]. The image noise is reduced in proportion to the increase of the voxel size and the beam projections. Previously published reports showed that the image noise of CBVT (MercuRay) was of a higher value than that of Helical CT, but it still had low noise properties [99, 100] .This is similar to a result in Hashimoto's study. It was reported that CBVT reduced artifacts and noise when compared with conventional CT [101]. He suggested that CBVT was strongly preferred as a diagnostic imaging tool for hard tissues of the maxillofacial region due to its image quality and low radiation dose when compared with conventional CT.

Today, the CBVT system is being widely used in the oral and maxillofacial surgery and implantology due to its advantages. Firstly, CBVT provides sub-millimeter spatial resolution, shorter scanning time, and less radiation dose. Secondly, CBVT system is designed with different FOVs. For example, the NewTom3G has three FOVs, 6", 9", and 12" depending on the area of interest and the i-CAT has two FOV consisting of 16

cm x13 cm and 16 cm x 22cm. The smaller the FOV used, the higher is the resolution of images obtained.

Surfaces of voxels in conventional CT can be as small as 0.625mm square, but their depth is usually from 1-2mm. CBVT provides voxel resolutions that are isotropic – equal in all three dimensions. This produces sub-millimeter resolution ranging from 0.4mm to as low as 0.125mm [69]. For this reason, images of the CBVT are much clearer than that of conventional CT.

In terms of radiology, the image quality of the CBVT system is much better than that of medical CT [68] because the CBVT system with about two line pairs per millimeter had approximately fourfold as much resolution as the medical CT [101]. Furthermore, tomographs of volume data can be collected in any planes from primary reconstruction.

Kobayashi et al [102] reported that there was significant difference in measurement error between the CBVT and spinal CT. As a result, with its valuable advantages, it is clear that CBVT is an imaging diagnostic tool more accurate than conventional CT and traditional modalities.

In terms of clinical application, Neugebauer et al reported that a number of nerve injuries were significantly reduced from 3 or 4 cases per year to 1 per year since CBVT has been used for diagnostic imaging [103]. This demonstrates that CBVT system has optimal benefits when compared to other diagnostic systems such as CT and conventional radiography. Additionally, the precise assessment of the mandibular canal associated with implant placement could reduce surgical and wound-healing time [103].

It was concluded that CBVT with its benefits is superior to medical CT.

At present, the medical CT system including helical/ spiral CT and multidetector CT has been used in clinical practice in both the medical and dental fields [57]. Before CBVT was launched into the dental market, medical CT was considered to be the best and most accurate diagnostic tool [2, 56, 81]. Spiral CT offers some benefits such as reduced scan time, improved, superior lesion detection, and optimized three-dimensional reconstruction, but it also has some disadvantages such as high radiation dosage and high cost. Also, the resolution of conventional CT is lower than that of CBVT, especially in the axial scanning due to limitations in accurate movements of the patient table and focal spot size [66, 99]. Regarding the accuracy, a measurement error of 5% in evaluating clinical imaging should be clinically reliable in studies of conventional CT [98, 104].
Kim et al [105] stated that the vertical measurement of the reformatted cross-sectional images of conventional C T might be affected as the position of mandible changes in the CT gantry. Furthermore, the linear distance between the most superior border of the mandibular canal and the alveolar crest also increased as the angle between the CT scanning plane and mandibular plane increased because conventional CT scan reformatted a series of parallel helical slices and a small gap existed among parallel slices leading to an error [6].

Before CBVT appeared in the dental market, conventional CT was the most accurate method to assess the relationship between the mandibular canal and impacted lower third molars. [106, 107]. However, it should be noted that it may be an expensive procedure for patients and not always feasible for surgeons [106].

2. What is the difference between the NewTom3G and i-CAT machine?

The application software of these two units is quite similar and user-friendly. However, there are a few differences to be noted. In the NewTom3G, a marker tool is used to indicate the mandibular canal. This marker gives a better visualisation of the mandibular canal when compared with the visualisation in the i-CAT unit (Fig 24, page 45). In the i-CAT unit, the axial plane can be adjusted to obtain a balance for the right and left sides. These are manufacturers' differences which are not significant in clinical application.

Table 18 shows configuration and physical properties of the NewTom3G and i-CAT machines. Resolution of images using the i-CAT unit seems to be higher than that of the NewTom3G. The images displayed on the screen of the i-CAT unit are clearer than that of NewTom3G. This difference could be attributed to two factors. Firstly, the grey-scale of images of the i-CAT is 14 bit compared with 12 bit of the Newtom3G. Secondly, the image-detector of the i-CAT design is different from that of the NewTom3G. The image–detector of the i-CAT machine is an amorphous silicon flat panel, while the NewTom3G is an image intensifier/ CCD. [71, 75]. Certainly, due to limited knowledge in algorithms and physics about the CBVT system, it was proposed that explanation was speculative. It should be viewed with caution until further research answers the question 'why images of the i-CAT were clearer and more detailed when visualized on the screen than that of NewTom3G'.

Table 18. Configuration and physical properties [108, 109]

Configuration and physical properties	i-CAT	NewTom3G
X-ray Beam	Cone	Cone
Focal spot	0.5 mm	0.3 mm
Image Detector	Amorphous Silicon Flat Panel/ Caesium iodide Csl	Image intensifier/ CCD
Grey Scale	14 bit	12 bit
Voxel Size	0.4mm (typical), 0.2 mm (minimum)	0.2mm
Image Acquisition	Single 360 degree rotation	Single 360 degree rotation
Scan Time	20 second standard (options of 10, 20, 40)	5.6 - 36 seconds
Patient position	Seated	Supine
Field of View (scan dimensions)	16 cm x 13 cm; 16 cm (diameter) x 22 cm (height)	6", 9" and 12"
Primary Reconstruction	1 minute for standard 20 second scan	1 – 3minutes
Secondary Reconstruction	Real Time	Real time
Default parameters	120 kVp, 1-3 mA	110 kVp, 15 mA

Patient positioning

The patient is more comfortable with the seated position used with the i-CAT machine when compared with the supine position of the NewTom3G machine. The seated position is similar to that used in the panoramic system that patients have been familiar with for some time. Much more space is required for a supine NewTom3G machine when compared to an i-CAT unit. However, the NewTomVG, the next generation of the NewTom3G, is available with the seated patient positioning.

These differences between the Newtom3G and i-CAT are not important. It is more of a commercial factor in the market competition because in terms of the dental clinical applications both these units are of great value and not significantly different.

3. The course of the mandibular canal on right and left sides

Regarding the course of the mandibular canal on both right and left sides, the findings showed that the course of the mandibular canal in the bilateral mandible was not significantly different. This was demonstrated by analysing the course of the mandibular canal in three-dimensional aspects at cross-sectional images of distances measured, LC, BC, and IC. At each position measured, the relationship between the mandibular canal and the mandible in the three – dimensional space with the lingual, buccal, and inferior aspects was evaluated. The findings showed that the course of the mandibular canals on both sides was not significantly different.

- BC distances measured on the right side were larger than those on the left side at the region of the first and second molars, but smaller at the region

of the third molar, however these differences have no significance on either side.

- LC distances measured on the right side at the regions of the first, second and third molars were larger than those on the left side except at the regions of the second and third molars as shown in the NewTom3G.
- IC distances measured on the right side at the regions of the first, second and third molars were larger than those on the left side, except in the iCAT and manual measurement at the region of the first and third molars.

The findings showed in most cases, on average, the mean difference of distances measured at BC, LC, and IC ranged from 0.12 to 0.49 mm on the left and right sides. In particular, for LC distances measured at the third molar, the mean difference between right and left sides was considered to be a minimum of 0.07, 0.18 and 0.21mm for the NewTom3G, i-CAT and manual measurement, respectively.

In contrast, for IC distances measured at the third molar, the mean difference between right and left sides was considered to be a maximum of 0.83, 0.95 and 1.15 mm for the NewTom3G, i-CAT and manual measurement, respectively. However, all these differences were not significantly different between the left and right sides. It is concluded that the course of the mandibular canal on both sides is variable.

In the present study, the course of the mandibular canal was evaluated by focusing only on three sites at the regions of the first, second and third molar at intervals of 10mm. For this reason the course of the mandibular canal could not be accurately

predicted within each 10 mm measurement. Further research with closer intervals of 1 or 2mm, for instance, might validate the accuracy of the course of the mandibular canal.

4. Valuable references of measured variables

Table 19. Summary of distances measured in the correlation between the mandibular canal in the region of lower molars and the mandible on the Newtom3G and i-CAT.

Region	Measured variables	Right side		Left side	
The first molar	Mean (mm)	NewTom3G	i-CAT	NewTom3G	i-CAT
	AC	12.38	12.62	13.97	13.02
	BC	6.20	6.25	5.75	5.85
	LC	3.71	3.62	3.23	3.22
	IC	9.44	8.97	9.17	9.24
The second molar	AC	11.83	11.68	12.48	12.12
	BC	7.01	7.07	6.67	6.70
	LC	3.28	3.66	3.49	3.36
	IC	9.86	9.46	9.37	9.06
The third molar	AC	11.78	12.29	12.16	12.34
	BC	5.72	5.74	6.37	6.54
	LC	3.61	3.82	3.68	3.64
	IC	11.03	10.51	10.20	9.56

Table 19 summarized valuable references of the distances measured at the region of the first, second and the third molars on the NewTom3G and i-CAT machines. In this study, the findings showed the LC was the shortest distance, ranging from 3.22 mm (±0.82) to 3.82 mm (±0.97) in the relationship between the mandibular canal and the mandible in the lingual aspect of the buccolingual direction. In terms of dental clinical practice, the diameter of a bur in oral surgery is usually from 1.5 to 2.0 mm [32]. It could damage the IAN during surgery if information about relevant structures was insufficient. A CBVT scan is now preferred to exactly locate the IAN when planning surgery.

Regarding the distance measured from the alveolar ridge of the mandible to the superior border of the mandibular canal, Levine et al reported that the distance from the alveolar crest of the mandible to the superior border of the mandibular canal in the first molar of dentate patients was 17.4 mm [32]. In another study Frei reported that this distance was 13.9 mm (±2.66) at the region of mandibular molars of 50 edentulous patients. Additionally, Naitoh et al reported on average this distance was 13.97mm (±2.03) and 13.78 mm (±2.16) with 10 distances measured on three dry mandibles using the micro-CT and helical scan. In the present study, this distance was ranged from 12. 38 to 13.97 mm, including 70% of edentulous patients and 30% of dentate patients. This result was almost similar to the studies of Frei and Naitoh. However, it was different from Levine's report. The following factors could attribute to this difference.

- The alveolar resorption of the mandible could be significant after extracting mandibular molars.

- The author's research was carried out on dry mandibles leading to possible shrinkage.
- The size of the mandible might be different between the American and Vietnamese races.

Additionally, in Levine's study, on average, the canal was 4.9 mm from the buccal cortical margin and this distance was from 5.75 to 6.25 mm in the present study. From this, it was supposed that the bone width of the mandible in the bucco-lingual direction of Vietnamese may be slightly wider than that of the American. However, in order to corroborate this, further research should be carried out with the same criteria as the study mentioned.

5. How valuable is a panoramic radiograph?

As previously mentioned, panoramic radiographs have some disadvantages. They provide information of anatomic structures in two dimensions only. This limitation could be a problem in surgical procedures such as removing impacted teeth or placing implants where a three-dimensional radiograph should be required to avoid injury to adjacent anatomical structures such as the IAN. Another disadvantage of the OPG is that images are magnified and distorted. In particular, this relates to the focal trough where proper positioning of patients is important to diminish magnification and distortion. In some cases where the maxillary canines and third mandibular molars are impacted, these teeth are usually located out of the focal trough due to their rotation and lead to magnification or distortion of the image. Panoramic images can reduce image quality because of superimposition of other structures. In most cases, however the mandibular canal is

visualized on a panoramic radiograph. For a panoramic radiograph, in clinical practice, differences produced by the different machines are less severe than those caused by the incorrect positioning of the patient by the operator [110].

However, OPGs also have some benefits. Conventional and digital panoramic systems are available and have become an important diagnostic tool in daily clinical practice [57].With a digital panoramic machine, structures of interest such as maxillary sinuses, or the TMJ can be selected. A half panoramic radiograph may be preferred rather than a full panoramic radiograph thus minimizing exposure time and radiation dose for the patient.

For clinical assessment, a panoramic image is still useful as a primary diagnostic radiograph for evaluation of pre-surgical procedures as it provides the complete picture of the dento-facial structures.

In this study, the difference in distances measured between the panoramic and CBVT systems were from 1.19 to 2.29 mm (Table 14-16, pages 77-79). It is assumed that distances measured on an OPG are likely to be valuable for a clinical evaluation if distances are reduced approximately 1 or 2 mm, depending on the magnification of the panoramic machine used. The results of this study suggest that the best and safest level is a minimum of 2.30 mm between the tip of an implant placed and the mandibular canal. Moreover, magnification of panoramic radiographs varies from 20 to 30%. However, this factor also depends upon patient positioning which can lead to magnification and distortion of images. Even with optimal patient positioning, correlations between anatomic structures on a panoramic radiograph might also be altered because the x-ray beam of panoramic tomography is directed upwards around 7-8^{o} [57].

In another study, Frei et al reported that, with the correctly positioned patient, the vertical magnification of panoramic radiographs was 1.27 and it was reliable for the selection of implant length in clinical practice. Additionally, he further concluded that a panoramic radiograph provided sufficient information about the vertical bone height in the posterior mandible and could be used for placing dental implants.

Newberry et al reported [111] that the vertical magnification of panoramic radiographs was from 1.26 to 1.27 and maximum magnification of vertical value was up to 1.67 when it was measured from the alveolar ridge to the mental foramen. This appears to be feasible for clinical use when the measurement of vertical distance is correctly calibrated. Moreover, in order to not damage the mandibular canal in the vertical direction, a safe distance at least of 1-2 mm from the tip of a placed implant to the mandibular canal should be maintained during the surgery procedure [112].

Frei et al reported that two clinical cases had temporary paraesthesia of the lower lip and the skin area of the chin because the distance from the tip of implant to the mandibular canal was less than 1mm when it was measured on panoramic radiographs. He further stated that “the surgeons hardly need the information from the cross-sectional images in treatment planning. It was supposed that this study included only standard implant cases where bone width was not the problem. In complex cases where great bone defects are present, an analysis with cross-sectional images is clearly recommended”.

In conclusion, the findings of the present study appear to fall in line with previous studies when the Orthophos machine was evaluated to compare with the CBVT system. More importantly, for the clinical use a decrease of approximately 2.30 mm in the

dimension of structures measured in two-dimensional panoramic radiograph should be strongly suggested.

Impacted third molars are often out of the focal trough due to rotated teeth and might lead to magnification and distortion of the image [82]. Furthermore, it is difficult to make a diagnosis in some cases where the apical tip of a third molar appears to contact the mandibular canal. In such cases, a CBVT radiograph should be preferred to obtain a more accurate diagnosis.

When using diagnostic radiographs for the inspection of the correlation between the mandibular canal and the impacted third lower molar, a conventional panoramic image is sufficient providing that these two structures are clear and separate. If not, a three-dimensional image should be requested [57].

However, in most cases involving the removal of impacted lower third molars, a panoramic radiograph is used in daily clinical practice instead of using medical CT or CBVT.

6. Case report

In the present study, the findings showed that LC is the smallest distance in all aspects of the relationship between the mandibular canal and the mandible (from 3.22mm to 3.82mm). Therefore, in terms of dental practice, dentists should particularly pay attention when making a surgical decision associated with the lingual aspect of the lower molar region. An injury of the mandibular canal due to incorrect placing of dental implants can prevent osseointegration or lead to sensory dysfunction [57]. The case reported below is an example of this (Fig 42).

It can be seen on the cross-sectional image in figure 42 that an implant was placed in the lower molar region towards the lingual aspect in the bucco-lingual direction and destroyed part of the mandibular canal. In Fig 42, LC distance measured was 3.23 mm, but the diameter of the implant was 5.31 mm. This indicates the use of this implant was not to be compatible for this patient, leading to damage the mandibular canal. The bone resorption level of mandible was severe in this case. The patient visited the Westmead Hospital with symptoms of sensory dysfunction of the IAN. A review of the medical history showed that when placing this implant, the dentist of this patient had solely used a panoramic radiograph for preoperative assessment. It is suggested that a CBVT scan should be requested to evaluate the LC distance to avoid undesirable injuries, especially in cases of severely atrophied mandibles.

Selection of the appropriate size and inclination of dental implants requires precise knowledge of the anatomy of the region of interest using three dimensional images as well as appropriate radiographs [5].

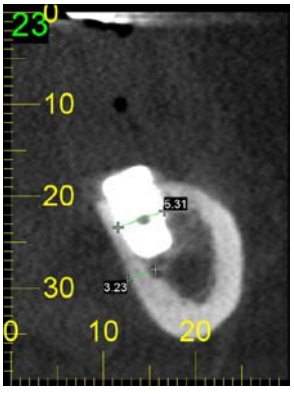

Figure 42. The cross-sectional image at the diameter position of the implant

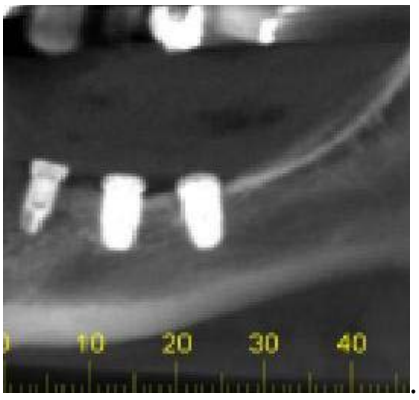

Figure 43. Part of the panoramic image showing the relationship between implants and the mandibular canal

(Courtesy of Oral Radiology Unit, Westmead Hospital, NSW, Australia).

Moreover, in the present study the findings showed there were significant differences between LC distances measured at edentulous areas from that of dentate areas. Further investigation about the mechanism of the bone resorption process is necessary to address this difference.

The finding also showed that the bone width of the mandible at the region of the first, second and third molars on the right side was slightly larger than that of the left side. It is not clear why that is, but it should be conceded that in the human body asymmetric structures are natural.

7. Implant size systems and application of software in dental clinicial practice

Presently, there are several implant products in the dental market. Each implant product is different from the other in design. Differences relevant to this study include the diameter and length of the implant which is chosen depending on the indications for the clinical cases. For example, the implant diameter of NobelActive^{TM} is 4.3mm [113]; and the Tapered Screw-Vent (Zimmer Dental) is available in 3.7, 4.7, and 6.0mm [114]. The most frequently used implants in the United States have a diameter of 3.75 mm and a length of 14 mm [46]. Longer implants with larger diameters loaded might minimize the bone stresses [115]. Anatomical structure is a further concerned in the selection of a suitable implant size.

Buser et al reported that when implants are placed in cancellous bone and are not embedded in the cortex bone, the tip of the implant might deviate up to 3.5 mm from the

desired position. This requires a wide safety zone of 3.5 mm around the planned implant tip position.

Recent software used for pre-surgical planning has rapidly developed to simulate implant surgery procedures and the mandible can be clearly seen in all spatial aspects by computed tools in this software. Currently, some products have been launched into the dental market such as Simplant, Nobel Biocare, BMi, 3D Diagnostix.com, Anatomage, Medical Modeling etc. For example, the two pictures below show a pre-implant planning of Simplant software that builds up implants in the posterior region of the mandible in relation to the mandibular canal after the data set of images was transferred to Simplant software.

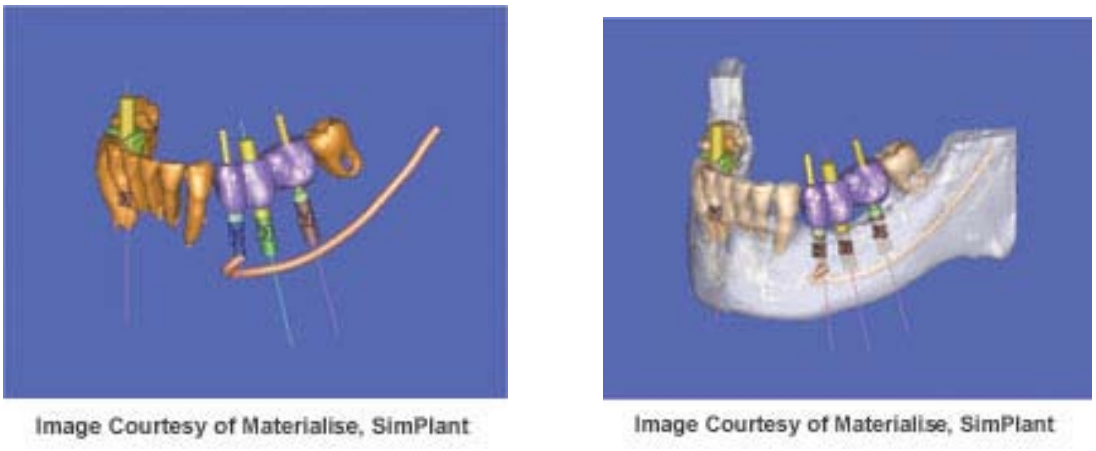

Figure 44. Information from CBVT was imported to appropriate software via DICOM.

8. Morphology of the mandible

For oral rehabilitation using implant placement, when dealing with a normally structured mandible, a panoramic radiograph can give useful information for diagnosis by the oral surgeon. A three-dimensional radiograph should be requested where mandibles are compromised or atrophic to obtain information in the bucco-lingual aspect to avoid the risk of an injured IAN.

In some cases, where completely edentulous mandibles were severely atrophied, it is essential to note that three-dimensional CBVT images should be preferred to obtain three- dimensional images, especially of the bone width in the bucco-lingual direction. Furthermore, not only for oral implants, but also for complex surgical procedures such as zygomatic implant placement or grafting, a CBVT scan should certainly be suggested in conjunction with software planning [82].

9. A number of limitations of this study

This study has a number of limitations. Firstly, the sample size was small and the study subjects were dry mandibles that had probably shrunk and certainly different from that of a patient. The mandibular canal of the patient is much more clearly visualized than that of the dry mandible [116].Thus the measurement error on the dry mandible could be higher than that of the patient. Secondly, the collected sample has not provided information associated with age and gender parameters that might cause a bias as well as a confounder. In summary, it is difficult to give a precise conclusive statement because this paper however is solely a pilot study as a platform for further research.

10. Further research

Further research with a larger sample size will be carried out to validate the accuracy of this study, using the data of patients stored in the Newtom3G machine at Sydney Dental Hospital, Australia. An evaluation of the mandibular canal associated with the age and gender of patients is being considered. The approach could be outlined as follows:

Method: from database of the images of one hundred adult patients would be used, consisting of 50 males and 50 females. The ages of the patients should be an important consideration. Data of these patients would be obtained from database of the NewTom3G machine stored in the computer workstation at Department of Oral Diagnosis and Radiology, Sydney Dental Hospital.

Aims:

- To evaluate the course of the mandibular canal at the molar regions of patients who were referred for scanning with the NewTom3G machine at Sydney Dental Hospital
- To compare the course of the mandibular canal on the left and right sides
- To answer the question - what measured figures from the research results can be considered to be valuable references for the dental practitioners
- To determine whether or not the age and gender of patients influence the course of the mandibular canal of the mandible.

Regarding to the direction of implants in the region of the lower molars, the author questions whether the direction of the implant should be parallel to the midline of the mandible or perpendicular to the alveolar ridge of the mandible. The ideas for research would be as follows:

A study sample is selected with the following criteria:

- Patients would be missing two to four of the first and second molars but at least missing two lower first molars included.

- Implants placed on the right side would be placed parallel to the midline of the mandible.
- Implants on the left side would be placed perpendicular to the alveolar ridge of the mandible.
- An assessment scale would be designed on both clinical and radiological findings to analyse the possibility of any differences.

The study design could be developed from this basic concept.

CONCLUSIONS

Currently, the CBVT system plays a key role and is the most accurate diagnostic tool in dental clinical applications such as pre-surgical and pre-implant planning. The differences in image quality as well as configuration and physical properties between the NewTom3G and i-CAT machines are not clinically significant in terms of dental diagnosis. Additionally, although the i-CAT may have been underestimated when compared with the NewTom3G in the aspect of measurement, visualization image is clearer than that of the NewTom3G. Again, these differences are not clinically significant. It is essential to note that the NewTom3G and i-CAT are recommended as excellent diagnostic imaging modalities for dental clinical applications.

The course of the mandibular canal in the regions of the first, second and third molars can be exactly determined based upon evaluation using CBVT. The distances measured as shown in table 19 can be considered as valuable references in terms of the

dental clinic. The course of the mandibular canal on the right and left sides is variable but not significantly different.

A conventional panoramic radiograph is still valuable in daily dental practice and can be a useful tool for assessment in pre-surgical and pre-implant procedures when used in combination with the skill, knowledge and experience of the surgeon.

It is conceded that neither conventional modalities nor CBVT can substitute for the skill, knowledge and experience of surgeons. However, it is clear that the excellent functions of CBVT combined with appropriate software plays an important role in the support of dental clinical applications, especially when evaluating pre-implant planning at the region of the mandibular molars.

In many cases, on OPGs, directions of the root of the lower premolars, the mesial root of the lower first molar and the upper first and second molars are shown to be nearly parallel to the midline mandible. In the mandibular molar region, the vertical direction of implant placement in relation to the mandibular canal a suitable position would be parallel to the midline of the mandible.

However, due to the limited scope of this study and the author’s limited knowledge of the physics and algorithms of the CBVT system as well as implantology, the explanations presented are speculative and therefore, should be viewed with caution until replicated with further studies.

REFERENCES

1. Ylikontiola L. Neurosensory disturbance after bilateral sagittal split osteotomy. *Oulu University Library* 2002.
2. Nasel C, Pretterklieber M, Gahleitner A, et al. Osteometry of the Mandible Performed Using Dental MR Imaging. *AJNR Am J Neuroradiol* 1999; **20**: 1221-1227.
3. Klinge B, Petersson A, Maly P. Location of mandibular canal: comparison of macroscopic findings, conventional radiography, and computed tomography. *Int J Oral Maxillofacial Implants* 1989; **4**: 327-332.
4. Naitoh M, Katsumata A, Nohara E, Ohsaki C, Ariji E. Measurement accuracy of reconstructed 2-D images obtained by multi-slice helical computed tomography. *Clin Oral Impl Res* 2004; **15**: 570-574.
5. Sukovic P. Cone beam computed tomography in craniofacial imaging. *Orthod Craniofacial Res* 2003; **6** (Suppl. 1): 31-36.
6. Winter AA, Pollack AS. Frommer H. H and Koenig L. Cone Beam Volumetric Tomography vs. Medical CT Scanners. *NYSDJ*. June/ July 2005.
7. Ylikontiola L, Moberg K, Huumonen S, Soikkonen K, Oikarinen K. Comparison of three radiographic methods used to locate the mandibular canal in the bucco-lingual direction before bilateral sagittal split osteotomy. *Oral Surgery Oral Medicine Oral Pathology Oral Radiology Endodontology* 2004; **93**: 736-742.
8. Claeys V. Bifid mandibular canal: literature review and case report. *Dentomaxillofacial Radiology* 2005; **34**: 55-58.
9. Kieser JPD, Kieser D, Hauman TDS. The Course and Distribution of the Inferior Alveolar Nerve in the Edentulous Mandible. *Journal of Craniofacial Surgery 2005*; **16**:6-9.
10. Hwang KMDP, Lee DMS, Song PMPH, Chung MDP. Vulnerability of the Inferior Alveolar Nerve and Mental Nerve during Genioplasty: An Anatomic Study. *Journal of Craniofacial Surgery* 2005; **16**:10.
11. Maegawa H, Sano K, Kitagawa Y, Ogasawara T, Miyauchi K, Sekine J, Inokuchi T. Preoperative assessment of the relationship between the mandibular third

molar and the mandibular canal by axial computed tomography with coronal and sagittal reconstruction. *Oral Surgery Oral Medicine Oral Pathology Oral Radiology Endodontology* 2003; **96**: 639-46.

12. Gabriel AC. Anatomy of the Teeth and Jaws. *University of Sydney Press*, 1965.
13. Bou Serhal C, van Steenberghe D, Quirynen M, Jacobs R. Localisation of the mandibular canal using conventional spiral tomography: a human cadaver study. *Clinical Oral Implant Research***.** 2001; **12:** 230-236.
14. Yoshida T, Nagamine T, Kobayashi T, Michimi N, Nakajima T, Sasakura H. Impairment of the inferior alveolar nerve after sagittal split osteotomy. *Journal of Cranio-Maxillofacial Surgery* 1989; **17**: 271-277.
15. Enciso R, Danforth RA, Alexandroni ES, Memon A, Mah J. The third molar impacted diagnostic with cone-beam computerized tomography. *International Congress Series* 2005; **1281**: 1196-1199. www.ics-elsevier.com.
16. Ellies L. Altered sensation following mandible implant surgery: a retrospective study. *J Prosthet Dent* 1992; **68**: 664.
17. van Steenberghe D, Lekholm U, Bolender C. Applicability of osseointergrated oral implants in the rehabilitation of partial edentulism: A prospective multicenter study on 558 fixtures. *Int J Oral Maxillofac Implants* 1990; **5**: 272.
18. Farronato G, Garagiola U, Farronato D, Bolzoni L, Parazzolid E. Temporary lip paraesthesia during orthodontic molar distalization: Report of a case. *Am J Orthod Dentofacial Orthop* 2008; **133**: 898-901.
19. Allard KUB. Paraesthesia - a consequence of a controversial root-filling material? A case report. *Int Endod J* 1986; **19**: 205-208.
20. Ruprecht A, Wagner H. Extrusion of endodontic filling material into the inferior alveolar canal. *J Can Dent Assoc* 1973; **54**: 683-685.
21. Steve M. Paraesthesia following endodontic treatment. *J Endod* 1976; **2**: 345-347.
22. Yashuhashi T, Nakagawa K, Matsumoto M, Kasahara M, Igarashi, Ichinohe T, Kaneko Y. Inferior alveolar nerve paraesthesia relieved by microscopic endodontic treatment. *Bull, Tokyo dent. Coll* 2003; **44**: 209-212.

23. Tsuji Y, Muto T, Kawakami J, Takeda S. Computed tomographic analysis of the position and course of the mandibular canal: relevance to the sagittal split ramus osteotomy. *International Journal of Oral and Maxillofacial Surgery* 2005; **34**: 243-246.
24. Susarla SM, Dodson TB. Preoperative computed tomography imaging in the management of impacted mandibular third molars. *J Oral Maxillofac Surg* 2007; **65**: 83-88.
25. Todd AD, Gher ME, Quintero G, Richardson AC. Interpretation of linear and computed tomograms in the assessment of implant recipient sites. *Journal of Periodontology* 1993; **64**: 1243-1249.
26. Hanazawa T, Sano T, Seki K, Okano T. Radiological measurements of the mandible: a comparison between CT-reformatted and conventional tomographic images. *Clin. Oral Impl. Res* 2004; **15**: 226-232.
27. Bartling R, Freeman K, Kraut RA. The incidence of altered sensation of the mental nerve after mandibular implant placement. *J Oral Maxillofac Surg* 1999; **57**: 1408-1410.
28. Theisen FC, Shultz RE, Elledge DA. Displacement of a root form implant into the mandibular canal. *Oral Surgery, Oral Medicine, Oral Pathology* 1990; **70**: 24-28.
29. Fanuscu MI, Chang TL. Three-dimensional morphometric analysis of human cadaver bone: microstructural data from maxilla and mandible. *Clinical Oral Implant Research* 2004; **15**: 213-218.
30. Schwarz MS, Rothman SLG, Rhodes ML, Chatetz N. Computed Tomography Part I. Preoperative assessment of the mandible of endosseous implant surgery. *Int J Oral Maxillofac Implants* 1987; **2**: 137-141.
31. Ulm CW, Solar P, Blahout R, Matejka M, Watzek G, Watzek G. Location of the mandibular canal within the atrophic mandible. *British Journal of Oral and Maxillofacial Surgery* 1993; **31**:370-375.
32. Levine MH, Goddard AL, Dodson TB. Inferior Alveolar Nerve Canal Position: A Clinical and Radiographic Study. *Journal of Oral and Maxillofacial Surgery* 2007; **65**: 470-474.

33. Patterson EJ. Bifid inferior alveolar canal. *Oral Surgery* 1973.
34. Langlais RP, Broadus R, Glass BJ. Bifid mandibular canals in panoramic radiographs. *J Am Dent Assoc* 1985; **110**:923.
35. Wong KSM, Jacobsen LP. Reasons for local anesthesia failures. *J Am Dent Assoc* 1992; **123**: 69.
36. Grover SP, Lorton L. Bifid mandibular nerve as a possible cause of inadequate anesthesia in the mandible. *J Oral Maxillofac Surg* 1983; **41**:177.
37. Yamada T, Kitagawa Y, Ogasawara T, Yamamoto S, Yamamoto S, Urasaki Y. Enlargement of mandibular canal without hypoesthesia caused by extra nodal non-Hodgkin's lymphoma. *Oral Surgery Oral Medicine Oral Pathology Oral Radiology Endodontology* 2000; **89**: 388-392.
38. Shapiro SD, Abramovitch K, van Dis ML, Skoczylas LJ, Langlais RP, Jorgenson RJ. Neurofibromatosis: oral and radiographic manifestations. *Oral Surg* 1984; **58**: 493-498.
39. Horswell BB, Holmes AD. Arteriovenous malformation in the mandible of a young child. *Aust N Z J Surg* 1988; **58**: 73-76.
40. Schenberg ME, Zajac JD, Collier NA, Brooks AMV, Reade PC. Multiple endocrine neoplasia syndrome-type 2b. *Int J Oral Maxillofac Surg* 1992; **21**: 110-114.
41. Mojaver NY, Sahebjamie M, Tirgary F, Eslami M, Rezvani G. Enlargement of mandibular canal with tongue paraesthesia caused by extra nodal B-cell Lymphoma: A case report .*Oral Oncology EXTRA* 2005; **41**: 97–99 .
42. Wang CC, Fleischli DJ. Primary reticulum cell sarcoma of bone with emphasis on radiation therapy. *Cancer* 1968; **22**: 994-998.
43. Barclay KJ. Enlarged mandibular canals. *Oral Surgery* 1971; **32**: 665-666.
44. Jacobs R, Aderiansens A, Vertreken K, Sutens P, van Steenberghe D. Predictability of a three-dimensional planning system for oral implant surgery. *Dental-maxillofacial Radiology* 1999; **28**: 105-111.
45. Van Assche N, van Steenberghe D, Guerrero ME, Hirsh E, Schutyser F, Quirynen M, Jacobs R. Accuracy of implant placement based on pre-surgical planning of

three-dimensional cone-beam images: a pilot study. *J Clin Periodontol* 2007; **34**: 816-821.

46. Himmlová L, Dostálová T, Kácovský A, Konvicková S. Influence of implant length and diameter on stress distribution: A finite element analysis. *The Journal of Prosthetic Dentistry* 2004; **91**:20-25.
47. Potter BJ, Shrout MK, Russell CM, Sharawy M. Implant site assessment using panoramic cross-sectional tomographic imaging. *Oral Surgery, Oral Medicine, Oral Pathology, Oral Radiology, and Endodontology* 1997; **84**: 436-442.
48. Jeffcoat M, Jeffcoat LA, Reddy SM, Berland L. Planning interactive implant treatment with 3-D computed tomography. *J. Am. Dent. Assoc* 1991; **122**: 40-44.
49. Weinberg LA. CT scan as a radiological database for the optimal implant orientation. *J. Prosth. Dent* 1993; **69**: 381-385.
50. Horiuchi M, Ichikawa T, Kanitani H, Wigianto A, Kawamoto N, Matsumoto N. Pilot-hole preparation for proper implant positioning and the enhancement of bone formation. J Oral Implantol 1995; **21**: 318-324.
51. Akca K, Iplikciolu H, Cehreli MC. A surgical guide for accurate mesio-distal paralleling of implants in the posterior edentulous mandible. *The Journal of Prosthetic Dentistry* 2002; **87**: 233-235.
52. Gaggl A, Schultes G, Karcher H. Navigational precision of drilling tools preventing damage to the mandibular canal. *Journal of Cranio-Maxillofacial Surgery* 2001; **29**:271-275.
53. Bou Sheral C, Jacobs R, Quirynen M, van Steenberghe D. Imaging technique selection for the preoperative planning of oral implants: a review of the literature. *Clinical Implant Dentistry and Related Research*. 2002; **4**: 156-172.
54. Mraiwa N, Jacobs R, van Steenberghe D, Quirynen M. Clinical assessment and surgical implications of anatomic challenges in the anterior mandible. *Clinical Implant Dentistry and Related Research*. 2003; **5**: 219-225.
55. Jensen O, Nock D. Inferior alveolar nerve repositioning in conjunction with placement of osseointergrated implants: A case report. *Oral Surgery, Oral Medicine, Oral Pathology* 1987; **63:** 263-268.

56. Reddy SM, Wang IC. Radiographic Determinants of implant performance. *Adv Dent Res* 1999; **13**: 136-145.
57. Jacobs R. Preoperative radiological planning of surgery in compromised patients. *Periodontology* 2003; **33**: 12-25.
58. Frei C, Buser D, Dula K. Study on the necessity for cross-section imaging of the posterior mandible for treatment planning of standard cases in implant dentistry. *Clin Oral Impl Res* 2004; **15**: 490-497.
59. Smith AC, Barry SE, Chiong AY, Hadzakis D, Kha LS, Mok SC, Sable DL. Inferior alveolar nerve damage following removal of mandibular third molar teeth. A prospective study using panoramic radiography. *Australian Dental Journal* 1997; **42**: 149-152.
60. Gray CF, Redpath TW, Smith FW, Staff RT. Advanced imaging: Magnetic resonance imaging in implant dentistry. *Clin Oral Impl Res* 2003; **14**: 18-27.
61. Gray CF, Redpath TW, Smith FW, Staff RT. Pre-surgical dental implant assessment by magnetic resonance imaging. *Journal of Oral Implantology* 1996; **22**: 147-153.
62. Hounsfield GN. Computed Medical Imaging. Nobel Lecture, 8 December 1979.
63. Cormack AM. Early two-dimensional reconstruction and recent topics stemming from it. Nobel Lecture, 8 December 1979.
64. Ning R, Kruger RA. Computer simulation of image intensifier-based computed tomography detector: vascular application. *Med Phys* 1988; **15**: 188-192.
65. Saint-Felix D, Picard C, Ponchut C, Romeas R, Rougee A, Troussert Y. Three-dimensional X-ray angiography: first in vivo results with a new system. *Proc SPIE* 1993; **1897**: 90-98.
66. Ning R, Wang X, Conover DL, Tang X. An image intensifier-based volume tomographic angiography imaging system. *Proc SPIE* 1997; **3032**: 238-246.
67. Shinoda K, Honda K, Matsumotoa K, Araib Y. Annual report of limited cone beam computed tomography (3D Accu-I-Tomo) from 3000 cases at Nihon University Dental Hospital in 2003. *International Congress* 2004 Series **1268**:1187–1191. www.ics-elsevier.com.

68. Arai Y, Hashimoto K, Iwai K, Shinoda K. Fundamental efficiency of limited cone-beam X-ray CT (3DX multi image micro CT) for practical use. *Dental Radiol* 2000; **40**: 145-154.
69. Scarfe WC, Farman AG, Sukovic P. Clinical Applications of Cone-Beam Computed Tomography in Dental Practice. *J Can Dent Assoc* 2006; **72**: 75-80
70. Farman AG, Scarfe WC. Dento-maxillofacial Cone-Beam CT for orthodontic assessment. *International Congress Series* 2005; **1281**: 1187-1190.
71. Rafferty MA, Siewerdsen JH. Intra-operative cone-beam CT for guidance of temporal bone surgery. *Otolaryngology - Head and Neck Surgery* 2006; **134**: 801-808.
72. Walker L, Enciso R, Mah J. Three-dimensional localization of maxillary canines with cone-beam computed tomography. *Am J Orthod Dentofacial Orthod* 2005; **128**: 418-423.
73. Siewerdsen JH, Jaffray DA. Cone-beam CT with a flat-panel image: Noise considerations for fully 3D computed tomography. *Proc SPIE Medical Imaging Visualization Display and Image-Guided Procedures* 2000; **3977**: 408-416.
74. Tantanapornkul W, Okouchi K, Fujiwara Y, Yamashiro M, Maruoka Y, Obayashi N. A comparative study of cone-beam computed tomography and conventional panoramic radiography in assessing the topographic relationship between the mandibular canal and impacted third molars. *Oral Surgery Oral Medicine Oral Pathology Oral Radiology Endodontology* 2007; **103**: 253-259.
75. Baba R, Ueda K, Okabe M. Using a flat-panel detector in high-resolution cone beam CT for dental imaging. *Dento-maxillofacial Radiology* 2004; **33**: 285-290.
76. Colbeth RE, Allen MJ, Day DJ, Gilblom DL, Harris R, Job ID. Flat panel imaging system for fluoroscopy applications. *Proc SPIE* 1998; **3336**: 376-387.
77. Yamada S, Umazaki H, Takahashi A, Honda M, Shiraishi K, Rudin S. Image quality evaluation of a selenium-based flat-panel digital X-ray detector system based on animal studies. *Proc SPIE* 2000; **3977**: 429-436.
78. Granfors PR, Aufrichtig R. Performance of a 41 x 41 cm2 amorphous silicon flat panel X-ray detector for radiographic imaging applications. *Med Phys* 2000; **27**: 1324-1331.

79. Verstreken K, Van Cleynenbreugel. JK, Marchal G, Nert I, Suetens B, Van Steenberghe D. Computed-assisted planning of oral implant surgery: a three-dimensional approach. *Int J Oral Maxillofac Impt* 1996; **11**: 806-810.

80. Fortin T, Coudert LJ, Chapleboux G, Sautot P, Lavellee S. Computed-assisted dental implant surgery using computed tomography. *J Image Guid Surg* 1995; **1**: 53-58.

81. Birkfellner W, Watzinger F, Wanschitz F, Ewers R, Bergman H. Calibration of tracking systems in a surgical environment. *IEEE T Med Imaging*1998; **17**: 737-742.

82. van Steenberghe D, Glauser R, Bloomback U, Anderson M, Schutyser F, Petterson A, Wendelhag I. A computed tomographic scan-derived customized surgical template and fixed prosthesis for flapless surgery and immediate loading of implants in fully edentulous maxillae: a prospective multicenter study. *Clinical Implant Dentistry and Related Research* 2005; **7**: 111-120.

83. Wanschitz F, Watzinger F, Schopper C, Ewers R, Birkfellner W, Figl M, Bergmann H, Patruta S, Kainberger F, Kettenbach J. Evaluation of accuracy of computer-aided intra-operative positioning of endosseous oral implants in the edentulous mandible. *Clinical Oral Implants Research* 2002; **13**: 59-64.

84. Tuzkymaz I, Tozum TF, Tumer C and Ozbek EN. Assessment of correlation between computerized tomography values of the bone, and maximum torque and resonance frequency values at dental implant placement. *Journal of Oral Rehabilitation* 2006; **33**: 881-888.

85. Loubele M, Jacobs R, Maes F, Denis K, White S, Coudyzer W, Lambrichts I, van Steenberghe D, Suetens P. Image quality *vs* radiation dose of four cone beam computed tomography scanners. *Dentomaxillofacial Radiology* 2008; **37:** 309 - 319.

86. Ludlow JB, Davies-Ludlow LE, Brooks SL, Howerton WB. Dosimetry of 3 CBCT devices for oral and maxillofacial radiology: CB Mercuray, NewTom 3G, and i-CAT. *Dentomaxillofacial Radiology* 2006; **35**: 219-226.

87. Mohl ND, Zarb GA, Carlsson GE, Rugh JD. *A Textbook of occlusion*, Chicago: Quintessence, 1988.

88. www.qrverona.it.
89. Guidelines for using the NewTom3G at Sydney Dental Hospital, Australia.
90. Farman AG, Scarfe WC. Development of imaging selection criteria and procedures should precede cephalometric assessment with cone-beam computed tomography. *American Journal of Orthodontics and Dentofacial Orthopedics* 2006**; 130**: 257-265.
91. Bartling SH, Majdani O, Gupta R, Rodt T, Dullin C, Fitzgerald PF, Becker H. Large scan field, high spatial resolution flat-panel detector based volumetric CT of the whole human skull base and for maxillofacial imaging. *Dentomaxillofacial Radiology* 2007; **36**: 317-327.
92. Feldkamps LA, Davis LC, Kress JW. Practical cone-beam algorithm. *J Opt Soc Am* 1984; **1**: 612-619.
93. Lascala CA, Panella J, Marques MM. Analysis of the accuracy of linear measurement obtained by cone beam computed tomography (CBCT-NewTom*) Dentomaxillofacial Radiology* 2004; **31:** 291-294.
94. Stratemann SA, Huang JC, Maki K, Miller AJ. Comparison of cone beam computed tomography imaging with physical measurements. *Dentalmaxillofacial Radiology* 2008; **37:** 80-93.
95. Tamas F. Position of the mandibular canal. *Int J Maxillofac Surg* 1987; **16**: 65-69.
96. Feifel H, Reidiger D, Gustorf AR. High resolution computed tomography of the inferior alveolar and lingual nerves. *Neuroradiology* 1994; **36**: 236-238.
97. Howerton WB, Mora AM. Advancements in Digital Imaging: What Is New and on the Horizon? *J Am Dent Assoc* 2008; **139**: 20-24.
98. Hilgers ML, Scarfe WC, Scheetz JP, Farman AG. Accuracy of linear temporomandibular joint measurements with cone beam computed tomography and digital cephalometric radiography. *Am J Ortho Dentofacial Orthp* 2005; **128**: 803-811.
99. Araki KL, Maki K, Seki K, Sakamaki K, Harata Y, Sakaino R, Okano T, Seo K. Characteristics of a newly developed dentomaxillofacial X-ray cone beam CT scanner (CB MercuRay): system configuration and physical properties. *Dentomaxillofacial Radiology* 2004; **33**: 51-59.

100. Endo M, Tsuno T, Nakamori N, Yoshida K. Effect of scattered radiation on image noise in cone beam CT. *Med Phys* 2001; **28**: 469-474.
101. Hashimoto K, Kawashima S, Kameoka S, Akiyama S, Honjoya T, Sawada K. Comparison of image validity between cone beam computed tomography for dental use and multidetector row helical computed tomography. *Dentomaxillofacial Radiology*; 2007, **36**, 465-471.
102. Kobayashi K, Shimoda S, Nakagawa Y, Yamamoto A. Accuracy in measurement of distance using limited cone-beam computerized tomography. *Int J Oral Maxillofac Implants* 2004; **35**: 525-528.
103. Neugebauer J, Mischkowski RA, Scheer M, Zoller JE. Comparison of cone-beam volumetric imaging and combined plain radiographs for localization of the mandibular canal before removal of impacted lower third molars. *Oral Surg Oral Med Oral Pathol Oral Radiol Endod* 2008; **105**: 633-642.
104. Waitzman AA, Posnick JC, Armstrong DC. Craniofacial skeleton measurements based on computed tomography: part I Accuracy and reproducibility. *Cleft Palate Craniofac J* 1992; **29**: 112-117.
105. Kim KD, Jeong HG, Choi SH, Hwang EH, Park CS. Effect of mandibular positioning on pre-implant site measurement of the mandible in reformatted CT. *Int J Periodontics Restorative Dent*. 2003; **23**: 177-183.
106. De Melo Albert DG, Gomes ACA, Egito Vasconcelos BC, de Oliveira Silva ED,Holanda GZ. Comparison of Orthopantomographs and Conventional Tomography Images for Assessing the Relationship Between Impacted Lower Third Molars and the Mandibular Canal. *Journal of Oral and Maxillofacial Surgery* 2006; **64**:1030-1037.
107. Lindh C, Peterson A, Kingle B. Measurements of distances related to the mandibular canal in radiographs. *Clin Oral Implants Res* 1995; **6**: 96.
108. Farman AG, Levato CM, Scarfe WC. A primer on Cone Beam CT, towards voxel vision: Continuing Education Program of Faculty of Dentistry, the University of Sydney. Sydney 15 August, 2007 (Presenter: Dr. William C. Scarfe)

109. Arnheiter C, Scarfe WC, Farman AG. Trends in maxillofacial cone-beam computed tomography usage. Oral Radiol 2006; 55-60. (Japanese society for Oral and Maxillofacial Radiology and Springer-Verlag 2006).
110. Coombs MI. Diagnostic imaging of the temporomandibular joint [Masters Thesis]. Faculty of Dentistry, the University of Sydney 1986.
111. Newberry J, Kozai Y, Chen CSK, Hollender L. Morphometric analysis comparing panoramic radiography to Cone Beam Computed Tomography. *Oral Surgery Oral Medicine Oral Pathology Oral Radiology Endodontology* 2008; Volume **105:** *Number 4, Abstracts e57.*
112. Buser D, von Arx T. Surgical procedures in partially edentulous patients with ITI Implants. *Clinical Oral Implant Research* **II** (Suppl) 2000; 83-100.
113. http://www.nobelbiocare.com
114. http://www.calcitek.com/news_press2008ArtA999.aspx
115. Lobbezoo F, Brouwers JEIG, Cune MS, Naeije M. Dental implants in patients with bruxing habits. *Journal of Oral Rehabilitation* 2006; **33**: 152-159.
116. Brooks SL, Beason RC, Sarment D, Sukovic P. Implant imaging with the I-CAT(R) cone-beam CT - a progress report. *International Congress Series* 2004; **1268:**1184-1186.www.ics-elsevier. com.
117. Okano T, Harata Y, Sugihara Y, Sakaino R, Tsuchida R, Iwai K, Seki K, and Araki K. Absorbed and effective doses from cone beam volumetric imaging for implant planning. *Dentomaxillofacial Radiology* 2009; 38: 79-85.
118. http://www.ctscan.co.uk/products/icat/ct_vs_cbct.html.
119. White S C, Pharoah M J. Oral Radiology: Principles and Interpretation, fifth edition 2004 Mosby 255.
120. http://www.aadmrt.com/currents/brooks_winter_05_print.htm
121. http://www.qrverona.it/htm/QR_NewTom3g_set%20frame3gen.htm#dose
122. http://www.precisiondx.com/download/radiation.pdf
123. Scarfe WC, Farman AG. Cone beam computed tomography: A paradigm shift for clinical dentistry. *Australian Dental Practice* July/ August 2007; 102-110.